

AD-A101 100

NAVAL POSTGRADUATE SCHOOL MONTEREY CA
EXPERIMENTAL STUDY OF NOISE PRODUCED BY AN UNDERWATER ACOUSTIC --ETC(IU)
JUN 81 C T KELLY

F/6 20/1

NL

UNCLASSIFIED

1 OF 1
AD A
10100

END
DATE
FILED
7-8-1
DTIC

AD A100700
ORIGINATOR

REF ID: A6711
NAVAL POSTGRADUATE SCHOOL
Monterey, California



THESIS

S-100-100-100
JUL 8 1981
A

6) EXPERIMENTAL STUDY OF NOISE PRODUCED BY
AN UNDERWATER ACOUSTIC BUBBLE SCREEN

by

Clark Thomas Kelley

17 June, 1981

Thesis Advisor: O. B. Wilson, Jr.

Approved for public release; distribution unlimited

DNC FILE COPY

Unclassified

SECURITY CLASSIFICATION OF THIS PAGE (When Data Entered)

REPORT DOCUMENTATION PAGE		READ INSTRUCTIONS BEFORE COMPLETING FORM
1. REPORT NUMBER	2. GOVT ACCESSION NO.	3. RECIPIENT'S CATALOG NUMBER
		AD-A101100
4. TITLE (and Subtitle) Experimental Study of Noise Produced by an Underwater Acoustic Bubble Screen		5. TYPE OF REPORT & PERIOD COVERED Master's Thesis; June 1981
7. AUTHOR(s) Clark Thomas Kelley		6. CONTRACT OR GRANT NUMBER(s)
9. PERFORMING ORGANIZATION NAME AND ADDRESS Naval Postgraduate School Monterey, California 93940		10. PROGRAM ELEMENT, PROJECT, TASK AREA & WORK UNIT NUMBERS
11. CONTROLLING OFFICE NAME AND ADDRESS Naval Postgraduate School Monterey, California 93940		12. REPORT DATE June, 1981
14. MONITORING AGENCY NAME & ADDRESS (if different from Controlling Office) Naval Postgraduate School Monterey, California 93940		13. NUMBER OF PAGES 64
16. DISTRIBUTION STATEMENT (of this Report) Approved for public release; distribution unlimited		18. SECURITY CLASS. (of this report) Unclassified
17. DISTRIBUTION STATEMENT (of the abstract entered in Block 20, if different from Report) Approved for public release; distribution unlimited		18a. DECLASSIFICATION/DOWNGRADING SCHEDULE
18. SUPPLEMENTARY NOTES		
19. KEY WORDS (Continue on reverse side if necessary and identify by block number) Bubble screen, bubble screen noise, acoustic bubble screen design.		
20. ABSTRACT (Continue on reverse side if necessary and identify by block number) Measurements in the Naval Postgraduate School's anechoic water tanks were conducted to determine the acoustic noise in the frequency range twenty hertz to ten kilohertz associated with injecting air into the tank through perforations in a two inch diameter PVC pipe. The effective source level for a pipe having several rows of smaller holes is ten to fifteen decibels smaller over most of the band than for pipe having a single row of holes		

Unclassified

~~SECURITY CLASSIFICATION OF THIS PAGE/When Data Entered~~

20. cont.

which produces the same flow rate. The measurements also indicate that the dominant source of noise is that associated with bubble formation and that the second most important source is from ascending bubbles. The impetus for this work was to study various aspects of the problem of designing a sound insulating bubble screen for the Carr Inlet Range of the Puget Sound Naval Shipyard.

Accession For	
1. GEA&I	<input checked="" type="checkbox"/>
2. TAB	<input type="checkbox"/>
3. Unannounced	<input type="checkbox"/>
4. Verification	<input type="checkbox"/>
Distribution/	
Availability Codes	
5. Avail and/or Dist	Special
<i>A</i>	

Approved for public release; distribution unlimited

Experimental Study of Noise Produced by
an Underwater Acoustic Bubble Screen

by

Clark Thomas Kelley
Lieutenant, United States Navy
B.S.M.E., Auburn University, 1974

Submitted in partial fulfillment of the
requirements for the degree of

MASTER OF SCIENCE IN ENGINEERING ACOUSTICS

from the

NAVAL POSTGRADUATE SCHOOL
June, 1981

Author:

Clark T. Kelley

Approved by:

O.B. Wilson, Jr.
Thesis Advisor

James H. Sanders
Co-Advisor/Second Reader

J.N. Dyer
Chairman, Department of Physics and Chemistry

William M. Tolles
Dean of Science and Engineering

ABSTRACT

Measurements in the Naval Postgraduate School's anechoic water tanks were conducted to determine the acoustic noise in the frequency range twenty hertz to ten kilohertz associated with injecting air into the tank through perforations in a two inch diameter PVC pipe. The effective source level for a pipe having several rows of smaller holes is ten to fifteen decibels smaller over most of the band than for pipe having a single row of holes which produces the same flow rate. The measurements also indicate that the dominant source of noise is that associated with bubble formation and that the second most important source is from ascending bubbles. The impetus for this work was to study various aspects of the problem of designing a sound insulating bubble screen for the Carr Inlet Range of the Puget Sound Naval Shipyard.

TABLE OF CONTENTS

I.	INTRODUCTION -----	9
II.	PROBLEM FORMULATION -----	14
III.	EXPERIMENTAL PROCEDURE -----	20
IV.	DATA -----	39
V.	DISCUSSION OF RESULTS -----	53
VI.	CONCLUSIONS AND RECOMMENDATIONS -----	58
	LIST OF REFERENCES -----	63
	INITIAL DISTRIBUTION LIST -----	64

LIST OF TABLES

I.	Resonant Radius for Air Bubbles in Water -----	15
II.	Projector at Center of Tank Calibration Data -----	27
III.	Projector on Left Side of Tank Calibration Data ---	28
IV.	Test Numbers -----	39
V.	One-Third Octave Band Analysis Raw Data -----	40
VI.	Bubble Screen Characteristics -----	49
VII.	Tabulated Power in One-Third Octave Bands for Signal+Noise -----	50
VIII.	Tabulated Power in One-Third Octave Bands for Signal Alone -----	51
IX.	Source Level for One-Third Octave Bands -----	52

LIST OF FIGURES

1a.	Velocity of Sound in Air-Water Mixtures -----	13
1b.	Reflection of Sound from Air-Water Mixtures -----	18
2.	Calibration and Measurement Equipment -----	21
3.	Tank Dimensions and Hydrophone Location -----	25
4.	Typical J-11 Current Response -----	25
5.	Pipe Configurations -----	30
6.	Bubble Screen Generation System -----	32
7.	Steady State Bubble Noise for Tests 1, 2, 3 -----	41
8.	Steady State Bubble Noise for Tests 4, 5, 6 -----	42
9.	Steady State Bubble Noise for Tests 7, 8, 9 -----	43
10.	Bubble Noise Components. (Same conditions as for test 6) -----	44
11.	Steady State Bubble Noise Test 1 (0-500 Hz) -----	45
12.	Steady State Bubble Noise Test 4 (0-500 Hz) -----	46
13.	Bubble Noise During Start Up -----	47
14.	Steady State Bubble Noise Test 1 (Screen flow rate 2.1 SCFM) -----	48
15.	Source Level for Tests 1 and 4 -----	59
16.	Source Level for Tests 3 and 5 -----	60

ACKNOWLEDGEMENTS

The author wishes to thank Mr. C. Henson and Mr. J. Kriebel of the Puget Naval Shipyard for suggesting this topic and for providing technical information in support of the project.

The author wishes to thank the Puget Sound Naval Shipyard for their financial support which enabled the purchase of necessary plumbing and measurement apparatus.

The assistance of Professor O. B. Wilson, Jr., often after normal working hours, and Professor J. V. Sanders, in areas of hydrodynamics, was greatly instrumental in the completion of this work.

I. INTRODUCTION

A. SCOPE

In this thesis some aspects of the feasibility of using a bubble screen to reduce noise interference at an acoustic range will be addressed. Specifically, determination of the noise produced by such a screen will be accomplished. Effects of emitter type and flow rate will be discussed.

B. BACKGROUND

The impetus for this work came from a need expressed by the Acoustic Range Division of the Puget Sound Naval Shipyard (PSNSY), Bremerton, Washington, for reducing ambient noise on their underwater test range at Carr Inlet arising from boat or rail traffic in and over nearby waters.

A vertical screen of gas bubbles used as an acoustical barrier in water to shield an area from undesirable outside noise sources is a concept that has been used for many years. The report of Carstensen and Foldy of their work during the 1940's on acoustic properties of bubble screens is a classic paper [Ref. 1]. A bubble screen has successfully been used in shipyards to insulate surrounding waters from the annoying sounds of high power search sonar during dock side tests. However, in reports we have studied, the frequencies of interest have been several thousands of hertz and higher.

Very little work has been directed toward the lower frequencies, which is an area of interest to those making noise surveys of ships whose noise spectra are of interest down to frequencies of a few hertz. Furthermore, in previous applications of bubble screens noise production has not been of primary concern.

The presence of numerous air bubbles in water has, in the case of bubble screening, the desirable effect of remarkably reducing the transmission of underwater sound. Upon striking the bubbly mixture, the incident sound energy can be reflected, absorbed or scattered depending on the composition and the geometry of the bubble screen and the sound frequency. For a screen consisting of a few bubbles small in diameter but uniform in size, the attenuation will be greatest at a particular frequency which can be explained by bubble resonance theories. However, if the bubble diameters vary considerably and the screen consists of many bubbles, the attenuation will be large over a much wider frequency range. In this case attenuation is explainable by the reduction of the specific acoustic impedance of the mixture, primarily due to the large resistive damping speed. In practice, attenuation usually results from both of these effects simultaneously [Ref. 1].

A dramatic effect of a gas bubble in water is the enhanced acoustic scattering cross-section which occurs when the sound frequency coincides with that of mechanical

resonance of the bubble [Ref. 3]. The resonance frequency of the bubble depends upon the diameter of the bubble and on the ambient hydrostatic pressure. Bubble stability, random bubble sizes during generation, and variation of bubble sizes during ascent limit the usefulness of resonance theories for screening lower acoustic frequencies.

The presence of air bubbles in water changes the mean density slightly but reduces the sound speed by a significant amount. Thus, there is a significant change in the specific acoustic impedance of the bubbly mixture compared to water. A one-percent fraction by volume of air in water can reduce the sound speed from a nominal 1500m/sec to about 100 m/sec [Ref. 4]. Thus, the acoustic impedance change can result in a significant acoustic reflection at the boundary between water and the bubbly mixture.

Another important effect in bubble screening is the generation of noise associated with the formation of bubbles and their oscillation as they migrate toward the surface. Some measurements with single bubbles indicate that most of the sound energy associated with the bubble arises at the orifice during bubble formation [Ref. 5].

So far as we know, radiated noise measurements have not been made on large numbers of bubbles, as from a bubble screen. Also, it is not clear that the results for single bubble formation can be applied properly to the case of many bubbles being formed near each other.

C. ENGINEERING CONSIDERATIONS

The basic engineering problem is how to design and use an underwater bubble screen at the Carr Inlet Acoustic Range to reduce unwanted noise caused by nearby boat and rail traffic. The examination lead to a number of questions which are pertinent.

Where should the screen be located?

At what depth should the screen be generated? How does the rise of say 450 feet effect the bubble size and the geometry of the screen.

If a screen is placed across the mouth of the inlet will a partial screen do the job?

What types of generators can be used to produce bubbles in water? Will corrosion and marine fouling interfere with the generation mechanism? If a manifold is chosen, how can air flow distribution be producted?

What thickness of screen and bubble concentration are required to produce an acoustically effective bubble screen? What size and distribution of bubbles are required.

How much noise does the screen itself inject into the environment?

What is the cost of the various options versus effectiveness?

The answers to the above questions each in turn depend upon the answer to one of the other questions in the group. As with many engineering problems no unique solution may

exist, but only some optimal solution based on compromises between cost and effectiveness. In order to facilitate problem solution several engineering assumptions had to be made. These assumptions affected the accuracy of the results and consequently the process was not a precision experiment. However, it is felt that useful conclusions can be drawn from the resulting data.

III. PROBLEM FORMULATION

A. PRELIMINARY

A primary concern was to choose a portion of the engineering problem that could be addressed effectively within the time constraints placed on this writer. The subtopic also had to be one that had a direct bearing on the overall solution and an early priority (i.e. must be answered before other questions can be answered). One such problem that fit the above requirements was determination of noise produced by the generation and existence of an acoustic bubble screen. Therefore, this topic is to be the main subject of this paper.

B. ASSUMPTIONS

In planning for measurements of noise generation from a bubble screen, it is necessary that certain characteristics must be estimated. The size and composition of a bubble screen as well as the size of the individual bubbles must be determined or an assumption must be made as to the range of values before proceeding further.

1. Resonant Bubbles

The phenomenon of resonance is responsible for the great efficiency of bubbles as scattering agents. However, bubbles of cross-sections large enough to be at resonance at

low frequencies would be difficult to generate, and, due to the hydrodynamics effect during migration, would soon break up into smaller bubbles as they rose. For example, see Table I for representative values [Ref. 6].

TABLE I. Resonant Radius for Air Bubbles in Water (cm)

Frequency (kHz)	Depth of Water (ft)			
	0	35	140	300
1	0.33	0.047	0.73	1.04
5	0.065	0.093	0.15	0.21
20	0.016	0.023	0.037	0.52

Furthermore, consistently producing bubbles of a specified diameter is not practical [Ref. 7]. At this point it was decided that resonance of the bubbles would not be effective as the primary mechanism for sound attenuation at the lower frequencies. However, any reduction of sound due to this phenomenon would be considered an additional benefit.

2. Reflection from the Screen

At the boundary of two dissimilar fluids the relative amounts of acoustic energy reflected and transmitted depends on the difference in the characteristic acoustic impedances of the fluids, the product of the densities and sound speed $\rho_1 c_1$ and $\rho_2 c_2$, of the two media [Ref. 8].

The problem of sound reflection from three or more fluids separated by parallel interfaces also depends on the changes in ρc and may also involve a standing wave in each of the internal layers. It seemed that the reflection due to acoustic impedance change would be the more promising approach to screening. Another thesis student, Lt. Ken Marr, is pursuing the detailed analysis. At this point it was assumed that since reflection theory would be the chosen approach, generation of a particular bubble size was not necessary.

3. Depth Considerations

It would have been desirable to make noise measurements with bubbles generated at a variety of water depths. However, since the only tank available for the measurements is 2.2m deep, the applicability of the results to other depths may be somewhat uncertain. If it is assumed that the primary mechanism for the generation of noise is the creation of the bubble [Ref. 5] then the pressure drop across the bubble creating orifice might be the controlling parameter. The hydrostatic pressure does affect the oscillation frequency of a bubble, so that an increase in the frequency of the maximum noise spectrum level might be expected at greater depth for the same size bubble.

4. Bubble Screen Concentration

The bubble reflection theory is based upon the impedance mismatch between the water and the bubble mixture. The greater the difference in ρc the higher the relative

amount of reflected energy as demonstrated by Eq. (1).

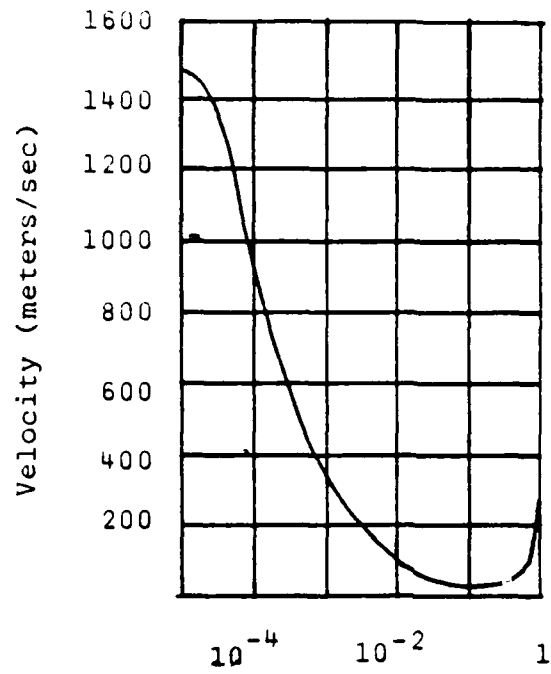
[Ref. 4, 8].

$$R = \frac{\rho_2 c_2 - \rho_1 c_1}{\rho_2 c_2 + \rho_1 c_1} \quad (1)$$

where R is the amplitude reflection coefficient for normal incidence. However, the relation is not linear. The greatest gain in reflected energy occurs as the fraction by volume of air in water is increased from about 5×10^{-4} to 10^{-2} . Increases in reflection for concentrations larger than 10^{-2} are minimal and do not justify the increased expenditure of air. For example a 10^{-2} ratio of air to water by volume gives 80 percent reflection as seen in Fig. 1a and 1b [Ref. 4]. Therefore, for planning purposes a bubble screen with concentration between 10^{-2} and 10^{-3} was chosen.

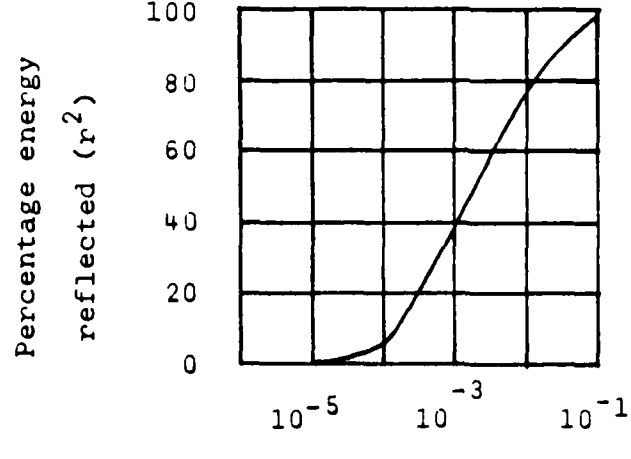
5. Bubble Rise Rates

One requirement for determining bubble concentrations is to know the speed as well as the bubbles' size. One source [Ref. 2] shows a graph of terminal velocities versus equivalent radius in still water. These numbers are useful only in a general sense that they show a general increase in terminal velocity with increasing radius with a region of rather constant terminal velocity from 0.1 to 0.6 cm radius. Since precise diameters could not be determined in the bubble screen experiments yet to be discussed, the rise rates were measured experimentally both in still water and in turbulent water (i.e. steady state screen). The assumption made was



Fraction by volume of air in water

Fig. 1 a. Velocity of Sound in Air-Water Mixtures
[Ref. 4]



Ratio of air to water (by volume)

Fig. 1 b. Reflection of Sound from Air-Water
Mixtures [Ref. 4]

that the bubbles reach terminal velocity rather quickly and then rise at a constant rate from that point. No attempt to predict increase in terminal velocity as the bubble expands due to decreasing pressure during ascent was made since the bubble diameters of produced bubbles were within the region of constant terminal velocity for a depth change of as much as five atmospheres. For a change of ten atmospheres the bubble radius can be expected to double which only causes an increase of 20 percent in speed. In turbulent water the same assumption was made.

6. Noise Measurement

The available acoustic measurement tank was not anechoic below 10 kHz, the region of interest. Therefore, measurement of acoustic power generated by the bubble screen required the assumption that an acoustic source of known power output placed in the tank to calibrate the hydrophones and mixing amplifier.

C. PARAMETER LIMITS

To keep the data to a manageable size the following limits for the various parameters were selected:

Bubble concentrations were to remain between 10^{-3} and 10^{-2} ratio of air to water by volume.

Actual air flow rates were to be 100 SCFM or less.

Air pressure differential between interior and exterior of pipe was to be five PSI or less.

III. EXPERIMENTAL PROCEDURE

A. SUMMARY

Calibration of the receiving equipment was accomplished by driving the J-11 projector with a known current in each one-third octave band from 25 Hz to 10,000 kHz. Also noted during this procedure was the relative shape of the received signal compared to the transmitted signal which gave a qualitative indication of the accuracy of the procedure.

Once the receiving hydrophones and mixing equipment had been calibrated, the projector was removed and the bubble generation manifold was installed approximately in the same location. Measurements were made to determine effects of holes size, number of rows of holes, differential pressure, and air flow rates upon the steady state noise produced by the pipe. Additionally, measurements under transient conditions were made in order to isolate and measure independently the noise produced by bubbles forming and ascending, bubbles ascending only and bubbles ascending and venting.

B. EQUIPMENT

Fig. 2 shows the equipment used for both the calibration phase and the measurement phase of the experiment. The same receiving equipment was used for the measurement phase while the projector transducer was replaced by the bubble

CALIBRATION AND MEASUREMENT
EQUIPMENT

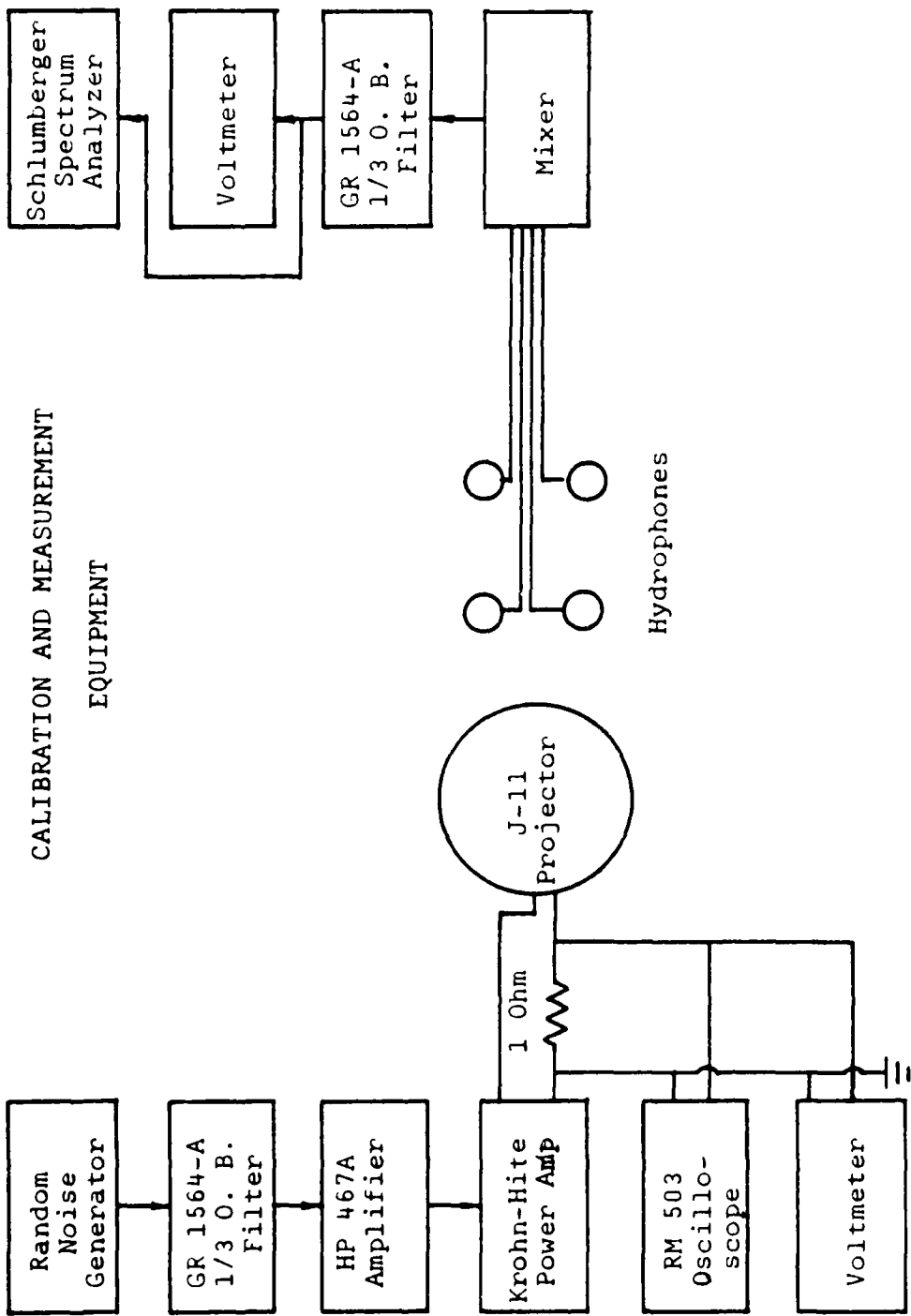


Fig. 2

screen as the sound source. A list of equipment is as follows:

1. Calibration Phase

- a. Tektronix RM 503 Oscilloscope
- b. Hewlett-Packard 3400 A RMS Voltmeter
- c. Krohn-Hite Wide Band DC-500 KC 50 Watt Amplifier

DCA-50R

- d. Random Noise Generator
- e. General Radio 1564-A Sound and Vibration Analyzer
- f. Hewlett-Packard 467A Power Amplifier
- g. USRD Type J-11 Transducer (Ser 102)
- h. One Ohm Resistor

2. Measurement Phase

- a. Four LC-10 Hydrophones (Serial numbers 2122, 1704, 1924, 2341)
- b. Shure Microphone Mixer
- c. General Radio 1564-A Sound and Vibration Analyzer
- d. Schlumberger Solartron 1510 Digital Spectrum

Analyzer

- e. Hewlett-Packard 3400 A RMS Voltmeter
- f. Hewlett-Packard 7035 B X-Y Recorder

3. Bubble Screen Apparatus

- a. 0-100 PSI Pressure Gauge
 - b. 0-80 PSI Pressure Gauge
 - c. RCM Industries 20-150- SCFM Direct Reading Flow-
- meter**

- d. DIGITEC Digital Thermometer
- e. Two-inch Schedule 40 PVC Pipe
- f. Various Valves, Elbows, and Fittings
- g. High Capacity Air Filter

C. CALIBRATION

The fact that the acoustic tank was not anechoic in the range of frequencies of interest prompted the investigators to do a cursory examination of the spatial characteristics of sound pressures in the tank. Some preliminary measurements using the J-11 transducer as a projector and a single LC-10 hydrophone indicated that location of the receiver within the tank indeed had a significant effect upon the level at the hydrophone. It was decided that more than one hydrophone would improve reliability of results. Therefore, four LC-10 hydrophones were used together and their outputs were mixed and then fed through a one-third octave filter and analyzer. Again trial measurements were taken to locate positions that provided a reasonably smooth frequency response. The resulting locations are shown in Fig. 3.

During the process of calibration and before the hydrophones were positioned as shown in Fig. 3, each hydrophone was assigned a channel on the mixer and was positioned in a central location each in turn. While in position, a test signal was generated on the J-11 and the output of each LC-10 was recorded on the spectrum analyzer. The gain of

each channel of the mixer was then in turn adjusted to give the most closely matching spectrum and peak dB level, so that each channel was matched to compensate for small differences in hydrophone sensitivity.

With the hydrophones in place and the channels matched, the calibration was continued by conducting a one-third octave band analysis on the sound and vibration analyzer. The procedure followed was to determine the current by measuring the voltage across the one ohm resistor in series with the projector as the one-third octave bands of random noise were injected into the J-11 transducer. The frequencies ranged from 25 Hz to 10 kHz. Simultaneously the voltage level within these bands was measured from the output of the mixer. Once this process was completed the free-field current response of the J-11 was applied at each frequency to determine source level by reading the current response level from Fig. 4 and adding $20 \log \frac{I}{I_{ref}}$ where $I = \frac{V}{R}$ and $R = 1$ ohm to the obtained value. The value of the power was then calculated from Eq. (2)

$$SL = 171.5 + 10 \log w \quad (2)$$

where SL = Source level

w = Power

to obtain the power in watts in the one-third octave band. Once the $10 \log w$ term is computed assuming that the process is linear over the range of values considered, a constant K

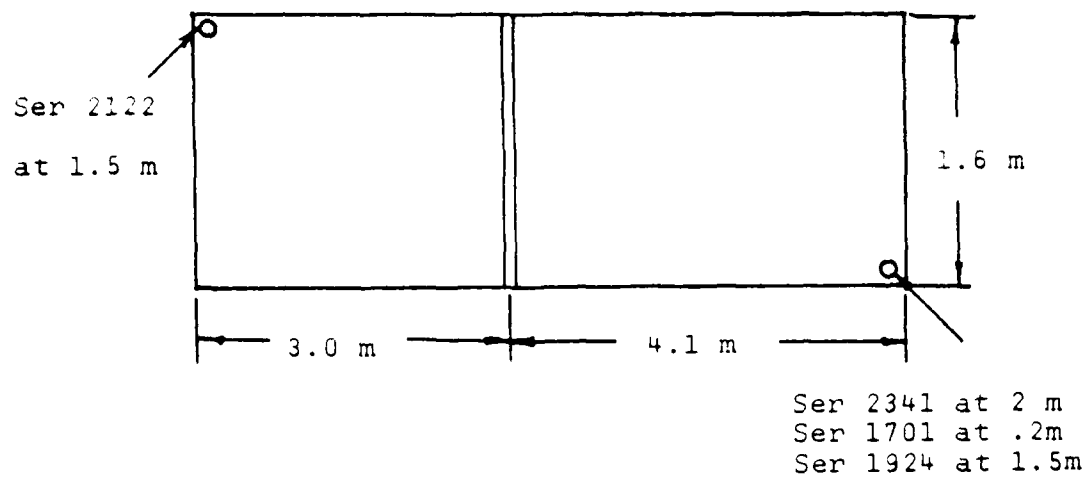


Fig. 3. Tank Dimensions and Hydrophone Locations

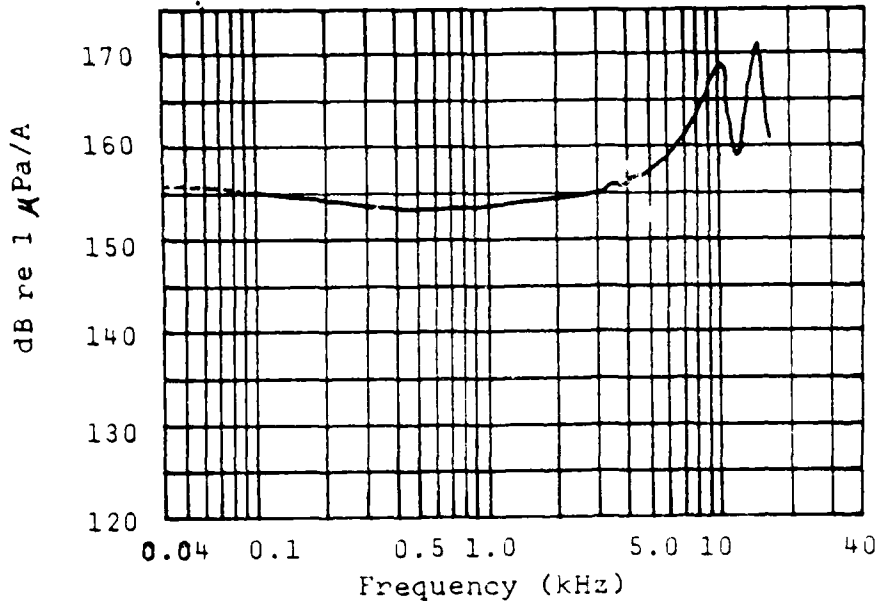


Fig. 4. Typical J-11 Transducer Current Response

can be determined for the purpose of calibrating the equipment to measure the power of an unknown source. This calibration procedure is also based on the assumption that the acoustic power output of the projector in this tank is the same as that which would be expected in the free-field case for the same input current. The accuracy of determining the constant K is further limited by the fact that the current response used for the J-11 projector was a nominal response typical for this type. A calibration curve for the projector used was not available. The value of K for each one-third octave was calculated from Eq. (3).

$$20 \log K = 20 \log \frac{V}{V_{ref}} + 10 \log \frac{W}{W_{ref}} \quad (3)$$

where V_{ref} = 1 volt

W_{ref} = 1 watt

The value of K was determined for three different projector locations along the width at the bottom center of the tank. These were center, left one-third and right one-third. The values of K were determined and averaged on an energy basis with an equal weighting given to each. The left and right values of K were virtually identical so that only the left side values were used. Tables II and III show both data and results.

Once the value of K had been determined it could be used to produce values of power generated by the acoustic bubble screen through use of Eq. (4).

TABLE II. Projector at Center of Tank Calibration Data

Freq.	SL	I	w	Hydro- phone	K	20 log K
Hz	dB re 1μPa/A	A	μ watt	mV	V W ^{1/2}	
25	155.0	0.04	36	0.3	0.5	-26.0
31.5	155.0	0.05	56	0.9	0.12	-18.0
40	155.0	0.05	56	1.7	0.23	-13.0
50	155.5	0.06	90	4.0	0.42	- 7.5
62.5	155.5	0.08	160	8.0	0.63	- 4.0
79.5	155.0	0.09	180	8.0	0.60	- 4.5
100	155.0	0.10	220	5.0	0.34	- 9.4
125	155.0	0.12	320	4.0	0.22	-13.0
157	154.5	0.13	340	2.0	0.11	-19.3
200	154.0	0.15	400	1.5	0.075	-22.5
250	153.5	0.16	405	1.5	0.075	-22.5
315	153.5	0.17	460	0.8	0.037	-28.6
400	153.5	0.16	405	0.8	0.040	-28.0
500	153.0	0.17	410	1.2	0.059	-24.5
625	153.0	0.17	410	1.2	0.059	-24.5
795	153.0	0.18	460	2.4	0.11	-19.0
1,000	153.5	0.18	515	2.4	0.11	-19.5
1,250	154.0	0.18	580	4.0	0.17	-15.6
1,570	154.5	0.18	650	6.0	0.24	-12.6
2,000	154.8	0.18	690	6.0	0.23	-12.8
2,500	155.0	0.18	725	5.5	0.20	-13.8
3,150	155.0	0.20	895	11	0.37	- 8.7
4,000	156.0	0.22	1,360	30	0.81	- 1.8
5,000	157.5	0.25	2,500	22	0.44	- 7.1
6,250	160.0	0.27	5,160	23	0.32	- 9.9
7,950	165.0	0.27	16,300	27	0.21	-13.5
10,000	169.0	0.29	47,300	100	0.46	- 6.7

TABLE III. Projector on Left Side of Tank Calibration Data

Freq.	SL	I	w	Hydro-phone	K	20 log K
Hz	dB re 1 μ Pa/A	A	μ watt	mV	$\frac{v}{w^2}$	
25	155.0	0.04	36	1.3	0.22	-13.3
31.5	155.0	0.04	36	1.7	0.28	-11.0
40	155.0	0.05	56	2.7	0.36	- 8.9
50	155.5	0.06	90	4.5	0.47	- 6.5
62.5	155.5	0.08	160	8.0	0.63	- 4.0
79.5	155.0	0.09	181	6.0	0.45	- 7.0
100	155.0	0.12	322	4.0	0.22	-13.0
125	155.0	0.13	378	4.0	0.21	-13.7
157	154.5	0.13	337	3.0	0.16	-15.7
200	154.0	0.14	349	3.0	0.16	-15.9
250	153.5	0.15	357	2.5	0.13	-17.6
315	153.5	0.16	406	3.0	0.15	-16.5
400	153.5	0.16	406	3.0	0.15	-16.5
500	153.0	0.17	408	2.0	0.10	-20.1
625	153.0	0.17	408	2.0	0.10	-20.1
795	153.0	0.18	458	3.0	0.14	-17.1
1,000	153.5	0.18	514	3.0	0.13	-17.6
1,250	154.0	0.18	576	5.0	0.21	-13.6
1,570	154.5	0.18	646	5.5	0.22	-13.3
2,000	154.8	0.18	693	5.7	0.22	-13.3
2,500	155.0	0.18	725	10	0.37	- 8.6
3,150	155.0	0.19	808	20	0.70	- 3.1
4,000	156.0	0.21	1,240	35	0.99	- 0.06
5,000	157.5	0.22	1,930	32	0.73	- 2.7
6,250	160.0	0.23	3,750	30	0.49	- 6.2
7,950	165.0	0.25	14,000	63	0.53	- 5.5
10,000	169.0	0.18	18,200	95	0.70	- 3.1

$$\text{Acoustic power} = \frac{(\text{Hydrophone voltage})^2}{K^2} \quad (4)$$

D. BUBBLE GENERATOR CONFIGURATIONS

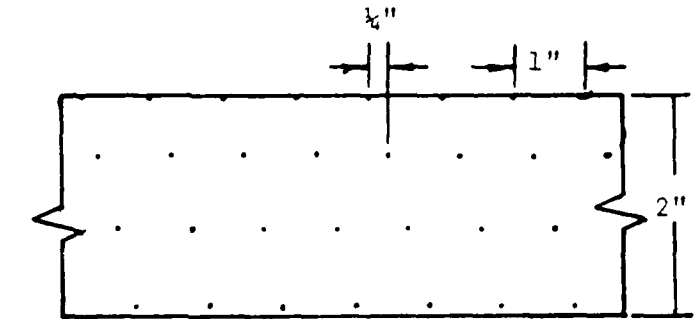
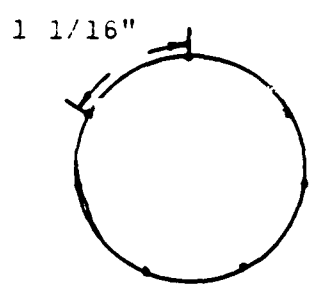
1. Type of Pipe

Three pipes of differing hole configurations were selected such that the bubble screen produced remained approximately within the previously mentioned concentration ratios. The first pipe was one consisting of holes arranged in seven rows equally spaced ($1\frac{1}{16}$ inch) around a two-inch schedule 40 PVC pipe. Holes were drilled with a #80 drill ($r = 0.007$ inch) and spaced one inch apart. In adjacent rows holes were staggered by one quarter inch as shown in Fig. 5. The pipe was 57 inches long to fit within the width of the tank and produced a 58 inch wide screen.

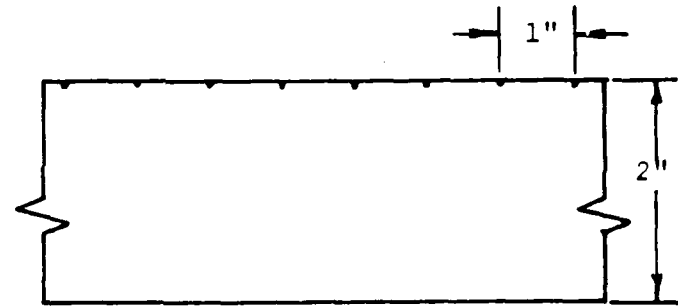
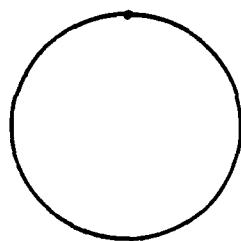
The second pipe was of the same dimensions and material, but with one row of #60 drill ($r = 0.02$ inch) holes spaced one inch apart in the top of the pipe and one hole at each end of the pipe on the bottom to facilitate purging any collection of water in the pipe. The total hole area for pipes one and two are approximately the same, and therefore flow rates were expected to be similar.

The third configuration was one row of #80 drill holes spaced at intervals of one inch on the top with one #60 drill hole on the bottom at each end for water removal.

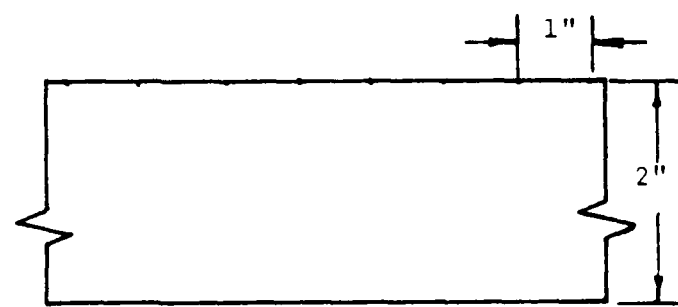
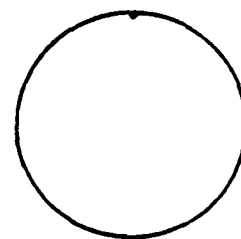
Each pipe was constructed such that it could be quickly and easily inserted for bubble generation. This was



Configuration One



Configuration Two



Configuration Three

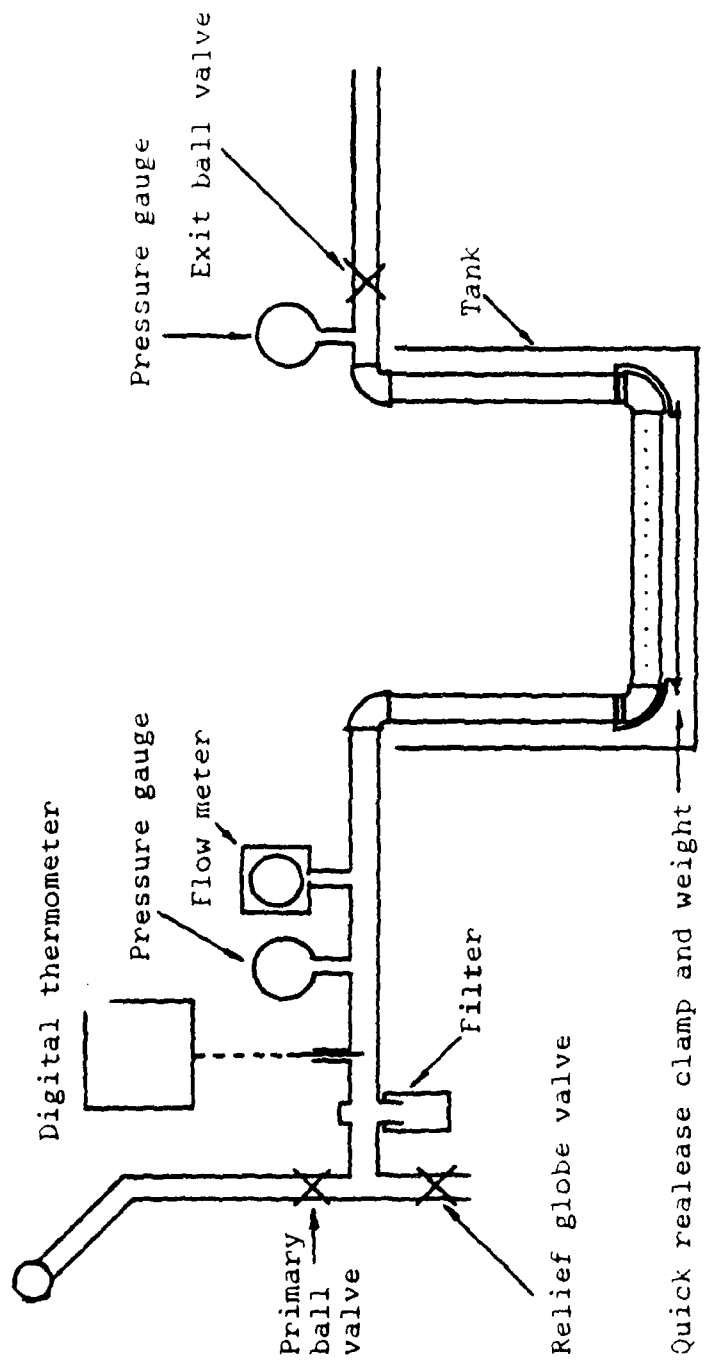
Fig. 5 Pipe Configurations

accomplished by cutting a groove in both ends for an "O" ring and using a clamping rod to prevent the pressure from forcing the pipe back out of its seat. See Fig. 6.

2. Flow Rate Measurements

Air flow rate was controlled by varying the differential pressure between the inside and the hydrostatic pressure in the water. The depth of the pipe was 6.76 feet from the water surface to the top of the pipe. Therefore the hydrostatic pressure in the water at the discharge pipe is very nearly 2.9 pounds per square inch gauge (PSIG). Pressures of 3.5, 5 and 7 PSIG were used throughout the experiment for convenience. The differential pressures were therefore 0.6, 2.1, and 4.1 PSI respectively.

Measurement of actual flow rates was accomplished by two methods. For the low flow rates (below the minimum for the flow meter) an approximate method for flow rate determination was utilized. A rectangular glass box (an aquarium) of dimensions, length 19.75 inches, width 10.31 inches, depth 11.88 inches and a volume of 1.40 cubic feet was filled with water and inverted so that no air was trapped within. The box was then moved to a position directly above the air screen to ensure that all bubbles within the segment covered were gathered in the container. Simultaneously a stop watch was started. When the glass tank was full of air the stopwatch was stopped, and the time was recorded. The volume divided by the time gives the air flow rate for that portion



BUBBLE SCREEN GENERATION SYSTEM

Fig. 6

of the screen. Assuming that the screen was uniform across the length of the pipe, the total flow was calculated by Eq. (5).

$$\text{Flow rate} = \frac{L_p}{W_A} \times \frac{V_A}{T} \quad (5)$$

where

L_p = length of screen = 4.83 feet

W_A = width of box = 0.86 feet

V_A = volume of box = 1.40 cubic feet

T = Time to fill

The method for high flow rates which were generated by opening the exit ball valve was to read the flow rate on the RCM direct reading flowmeter, record the temperature and pressure, and then calculate the actual flow rate by applying the following correction factor.

$$\text{True flow rate} = C \times \text{Meter reading} \quad (6)$$

where

$$C = \left(\left(\frac{P_a + 14.7}{P_c + 14.7} \right) \left(\frac{T_c + 460}{T_a + 460} \right) \right)^{\frac{1}{2}}$$

P = Actual gas pressure at entrance to meter PSIG

P_c = 80 PSIG

T_a = Actual gas temperature at meter °F

T_c = 80°F

D. EXPERIMENTAL MEASUREMENTS

A number of different measurements of bubble generated noise were made with each of the above pipe configurations

and pressures. The following remarks describe some of the characteristics of the system which influenced operating procedure. Also described below are measurements made under transient conditions which helped to understand the relative amounts of noise contributed by the various processes. That is generation, migration and venting of the bubbles.

1. Residual Water in Pipe

While the pipe was allowed to stand without air being supplied to it, water gradually filled the pipe as would happen if an installed screen were turned off. Measurement of the noise generated by water entering the pipe was made.

Once the pipe was filled with water it had to be forced back out of the pipe prior to producing a steady state bubble screen. A second set of measurements was made of the noise generated by producing a bubble screen from a pipe not completely purged of water.

2. Steady State Measurements

Four sets of measurements were made while the tubing was producing a continuous screen. These measurements were designed to simulate various portions of the pipe. In a long perforated pipe the air flow may be large near the supply end, and acoustic noise may arise from turbulent flow in the pipe. Some efforts towards measuring the noise generated with higher air flow was done by controlling the opening of an exit valve on the end of the perforated pipe. A hose was used to discharge the excess air to the exterior of the

room. These measurements were designed to determine the practical limit of air flow for a particular pipe diameter. Flow rates of less than 20, 50, 100, 150 SCFM gauge were chosen

3. Transient Measurements

Three more noise readings were taken with the intent of determining (1) the amount of noise produced by bubble creation at the orifice, (2) the amount of noise due to the bubbles venting at the surface, and (3) the amount of noise produced during the rise of the bubbles.

E. METHOD

1. Determination of General Trends

To determine the relative amount of acoustic power generated by a bubble injector that had not yet been purged of water was one objective. Each measurement condition was included in the process for this and subsequent procedures. The air supply valve was opened such that it produced the desired pressure and the initial transients were allowed to die out. Then before the water was forced completely out readings on the spectrum analyzer were taken and equipment settings were recorded. The GR 1564-A Sound and Vibration Analyzer was set to the all pass mode for this and subsequent readings so that the entire frequency range could be observed. This procedure produced data that could be analyzed for general trends.

Once the water was removed from the pipe, which could be observed by checking visually for air exiting from the bottom holes, steady state noise measurements were taken. Four different flow rates were introduced by adjusting the exit ball valve, see Fig. 5, to simulate various flow conditions within the pipe. This was accomplished by successively increasing pressure in the line and then bleeding off pressure with the exit valve until the desired flow rate was achieved. The above method ensured that no water re-entered the pipe during the process.

By maintaining air pressure within the pipe equal to the ambient water pressure the re-entrance of water was minimal. This fact allowed the bubble generator to be shut down for brief periods without affecting results taken immediately after restart. Therefore the following method was considered to give representative results about the source various noises within the screen.

Determination of the contribution to noise of the existing bubbles from the manifold was accomplished by stopping the bubble generation momentarily, allowing the turbulence and bubble motion to subside, and then resuming the bubble generation with exactly the same pressure as before. Opening the relief globe valve until the bubbles just stopped exiting and then closing it quickly worked about as well as opening the primary valve quickly to the correct pressure, hence both methods were used. The readings

on the spectrum analyzer were taken from the moment generation began until just before the bubbles broke the surface. A complete average was obtained by repeating the procedure many times until the averaging time on the spectrum analyzer had been reduced to zero and using the hold mode while re-setting the conditions.

Similarly, the effect of bubbles striking the surface was studied by starting an average on the spectrum analyzer just after the bubbles stopped exiting the orifices and suspending the average just before all the bubbles had risen to the surface. To ensure that bubbles were representative of the flow rate, the excess pressure was bled off quickly to ensure an abrupt stop of bubble flow from the pipe.

The rise of the bubbles themselves was also suspected as a noise generator. Therefore noise measurements were made during the time that bubbles were ascending but were neither exiting the pipe nor striking the surface. This was done by starting the bubble screen and running it for two seconds, then stopping bubble formation, and recording the noise from that moment until just before the bubbles broke the surface. Again, the process was repeated several times in order to achieve adequate average time.

2. Measurement of Steady State Power

The actual determination of acoustic power produced by the bubble screen was carried out by conducting a one-third octave band analysis of the hydrophone output signals with the GR 1564-A Sound and Vibration Analyzer. The readings were taken for each of three pipe configurations and each of the three pressures. The bubble screen was produced after the water was eliminated from the pipe and with the exit air valve closed.

3. Miscellaneous Readings

At both the 0-10 kHz and 0-500 Hz ranges ambient noise measurements were taken both on the spectrum analyzer and with the sound and vibration analyzer. Additionally a reading was taken when building air pressure had been depleted to approximately 7.5 PSI so that the primary ball valve could be completely opened to reduce air flow noise in the supply line. During the steady state operation of the screen general characteristics and approximate thickness of the screen for the various screen configurations were recorded.

IV. DATA

Table IV contains the test numbers for each combination of bubble generator and differential pressure. Table V contains the voltage readings for the one-third octave band analysis of each of the tests.

Spectral data from the spectrum analyzer were plotted using an X-Y recorder. Representative graphs have been included and general analysis of trends for all graphs have been included and general analysis of trends for all graphs will be discussed in the results section. See Fig. 7 through 14. The test numbers will be used for all further reference to pipe parameters. Tables VI, VII, and VIII contain data on screen characteristics and noise power. Table IX uses the data from Table VIII and Eq. 2 to show the results as an equivalent source level.

TABLE IV. Test Numbers

Pipe No.	Supply Pressure (PSIG)		
	3.5	5	7
1	1	2	3
2	4	5	6
3	7	8	9

Note: Test 10 was for noise

TABLE V. One-Third Octave Band Analysis Raw Data

Test Numbers

Freq.	1	2	3	4	5	6	7	8	9	10
Hz	mV									
25	0.10	0.09	0.10	0.07	0.10	0.10	0.09	0.01	0.10	0.10
31.5	0.15	0.18	0.15	0.14	0.13	0.15	0.10	0.09	0.09	0.13
40	0.15	0.10	0.12	0.20	0.15	0.15	0.10	0.09	0.10	0.10
50	0.20	0.20	0.23	0.60	0.25	0.22	0.20	0.19	0.20	0.19
62.5	0.65	0.65	0.65	1.0	0.70	0.70	0.65	0.65	0.65	0.65
79.5	0.20	0.15	0.18	1.1	0.40	0.45	0.14	0.13	0.13	0.15
100	0.20	0.12	0.15	0.90	0.60	0.55	0.10	0.11	0.16	0.13
125	0.20	0.17	0.18	1.3	1.0	1.0	0.20	0.25	0.20	0.22
157	0.40	0.33	0.33	0.90	1.3	1.0	0.26	0.28	0.26	0.23
200	0.60	0.60	0.60	1.3	1.5	1.5	0.45	0.45	0.42	0.55
250	0.20	0.15	0.20	1.0	1.1	1.0	0.16	0.15	0.15	0.13
315	0.14	0.13	0.20	0.35	0.50	0.40	0.15	0.14	0.13	0.14
400	0.10	0.10	0.10	0.15	0.30	0.25	0.12	0.11	0.13	0.10
500	0.10	0.11	0.10	0.15	0.25	0.30	0.13	0.13	0.14	0.10
625	0.09	0.11	0.11	0.15	0.30	0.28	0.11	0.11	0.12	0.07
795	0.10	0.14	0.15	0.24	0.60	0.50	0.11	0.13	0.13	0.07
1,000	0.09	0.14	0.18	0.20	0.50	0.50	0.13	0.18	0.15	0.06
1,250	0.08	0.14	0.20	0.23	0.70	0.55	0.17	0.19	0.23	0.06
1,570	0.08	0.20	0.22	0.23	0.70	0.70	0.18	0.22	0.35	0.05
2,000	0.07	0.16	0.22	0.30	1.3	1.3	0.27	0.35	0.80	0.05
2,500	0.06	0.18	0.30	0.55	3.0	2.8	0.45	0.70	1.5	0.05
3,150	0.07	0.25	0.55	1.6	8.0	7.0	1.2	2.0	4.5	0.05
4,000	0.09	0.45	1.0	1.8	8.0	6.5	1.4	2.0	5.5	0.06
5,000	0.14	0.65	1.8	1.4	5.0	4.2	1.0	1.5	4.5	0.06
6,250	0.30	0.50	0.90	0.60	2.0	0.45	0.70	2.0	0.07	
7,950	0.30	0.50	0.65	0.55	1.0	1.2	0.32	0.48	1.3	0.09
10,000	0.20	0.40	0.40	0.40	0.50	0.50	0.23	0.40	0.75	0.11

f₀

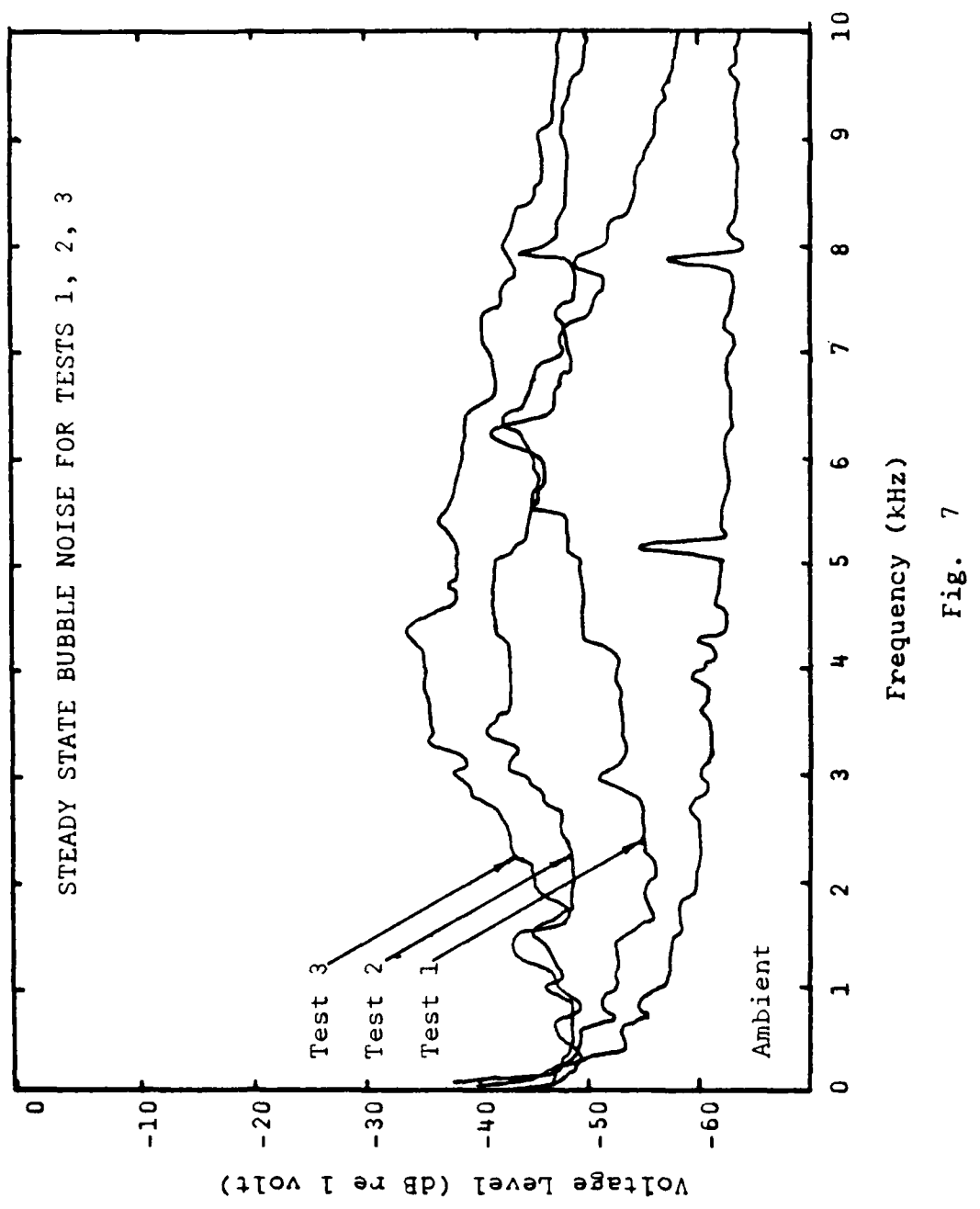


Fig. 7

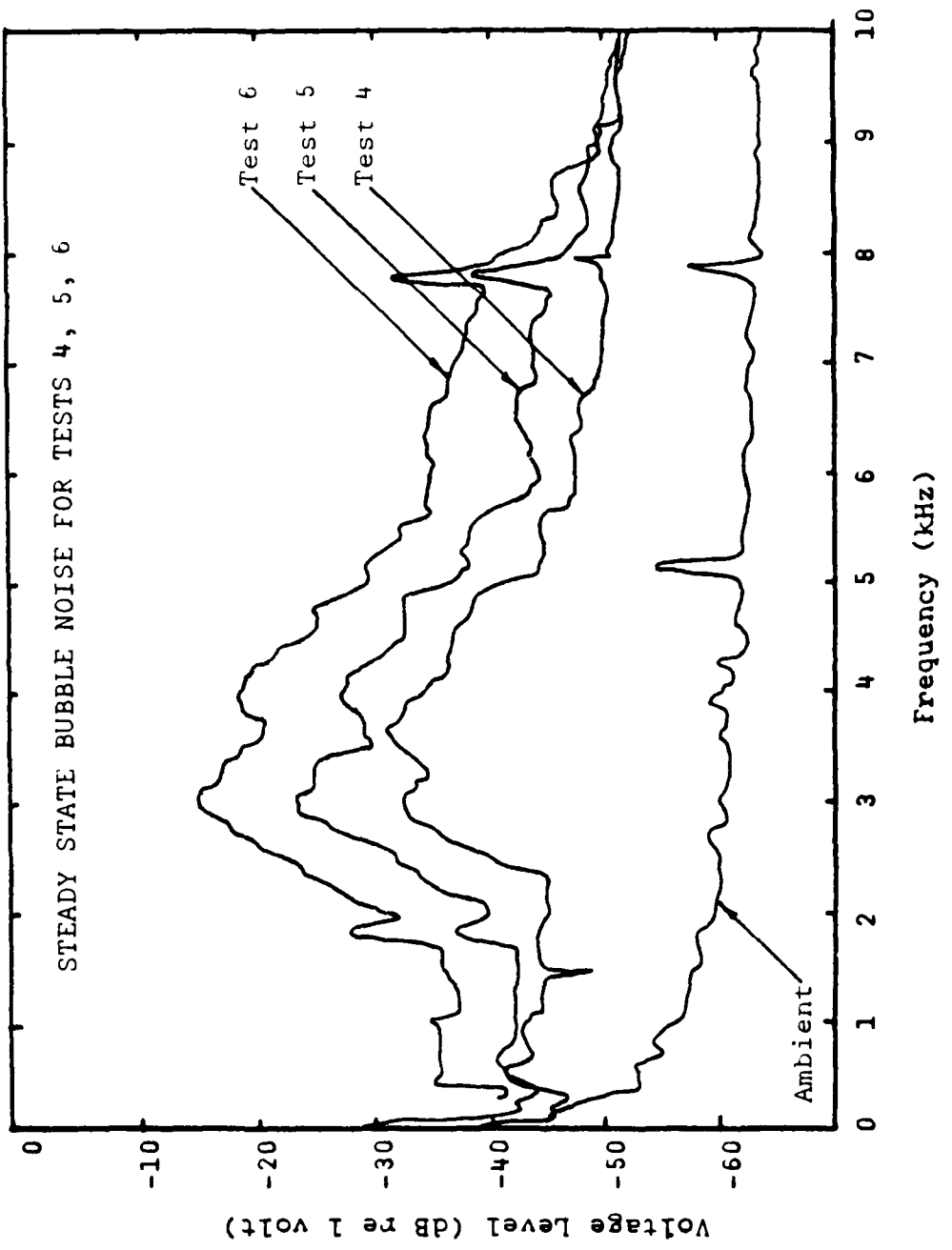


Fig. 8

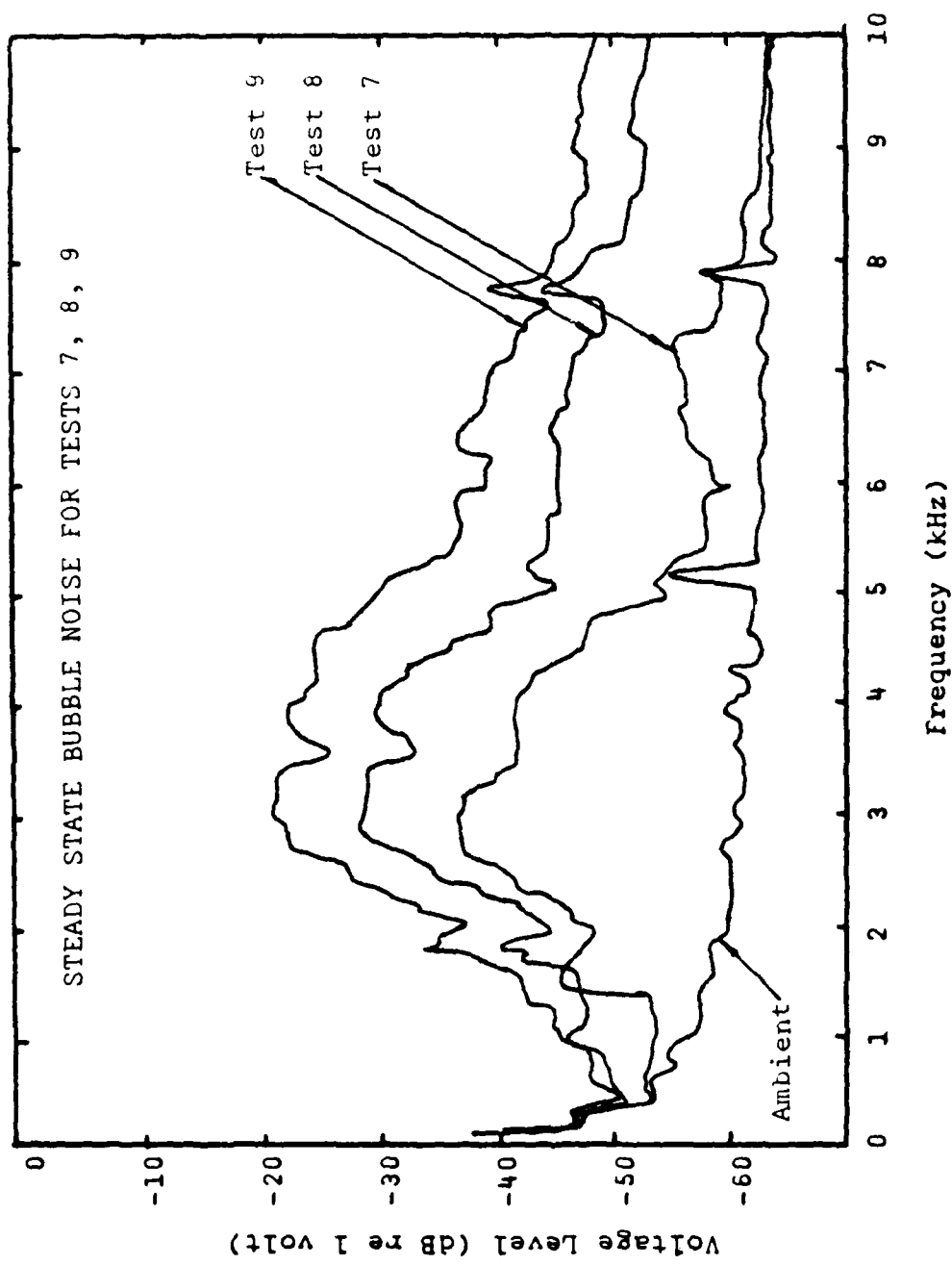


Fig. 9

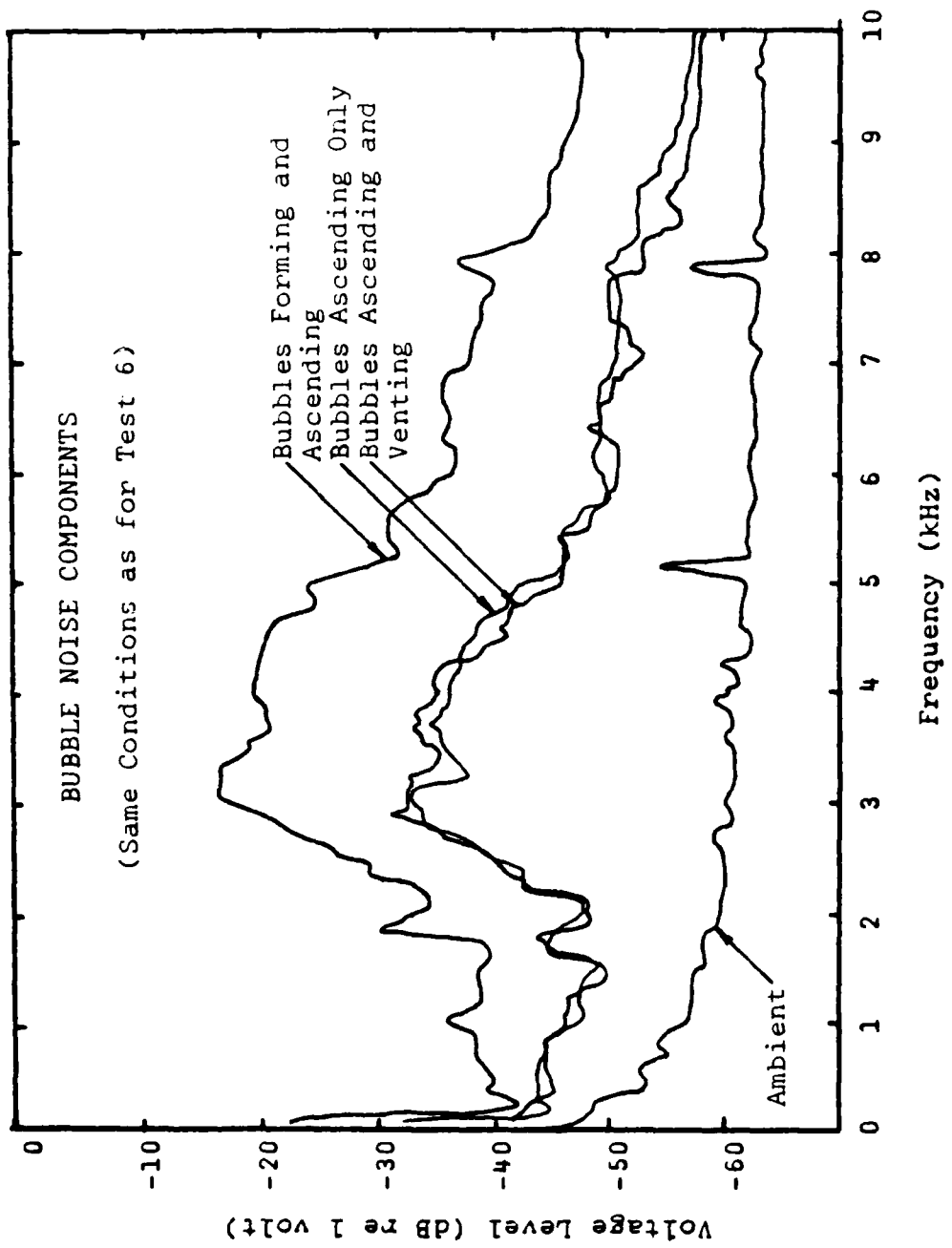


Fig. 10

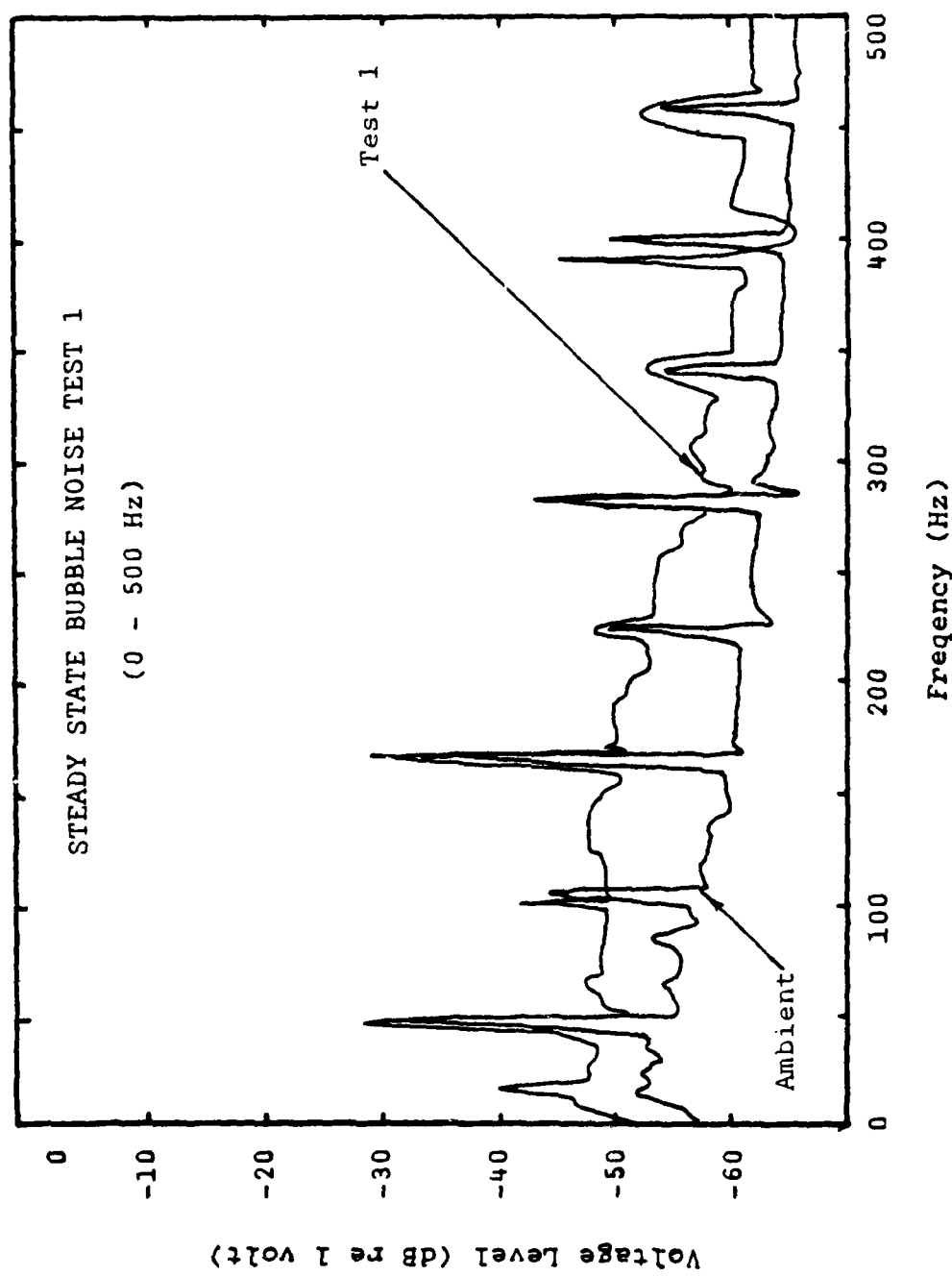


Fig. 11

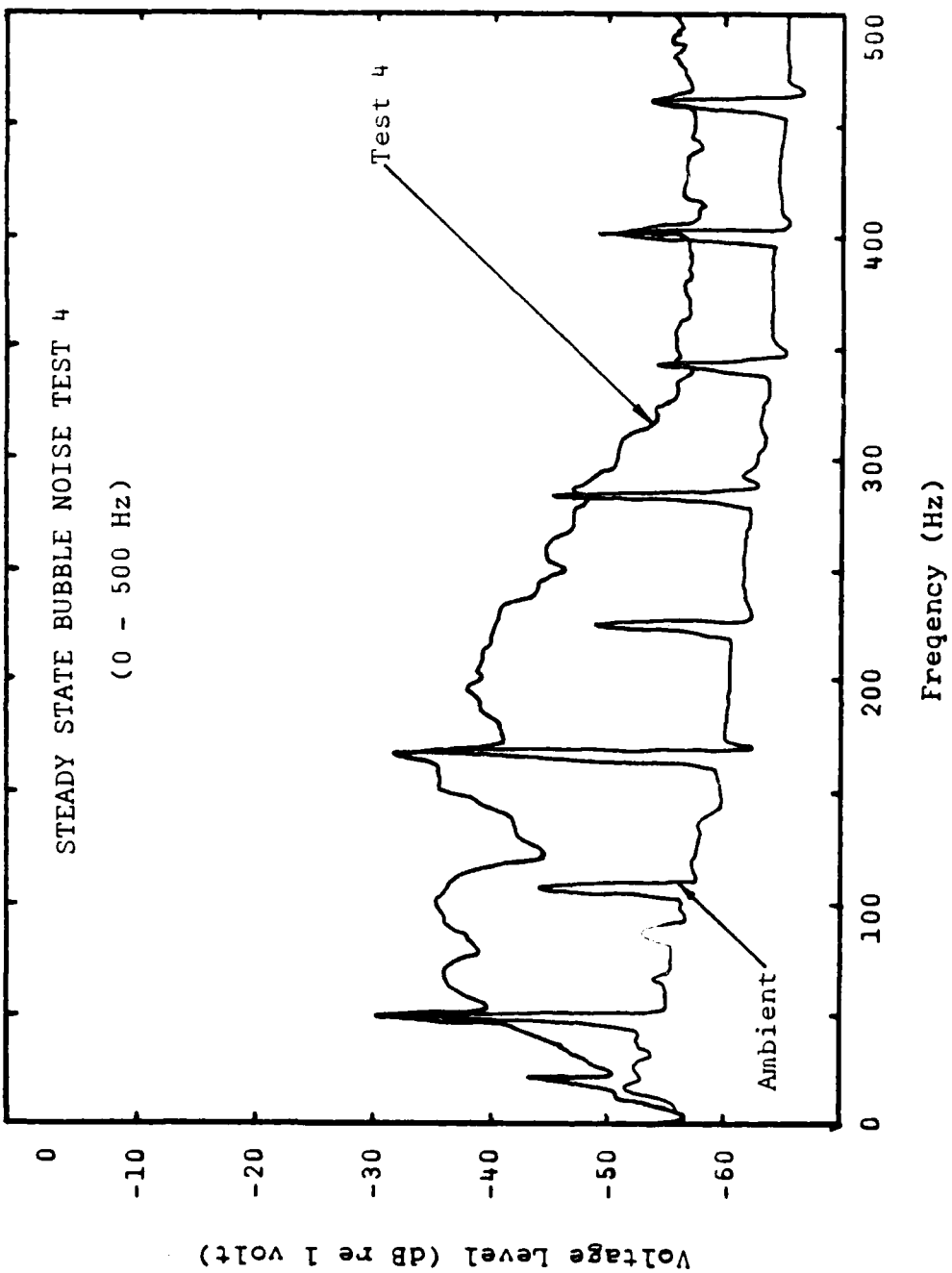


Fig. 12

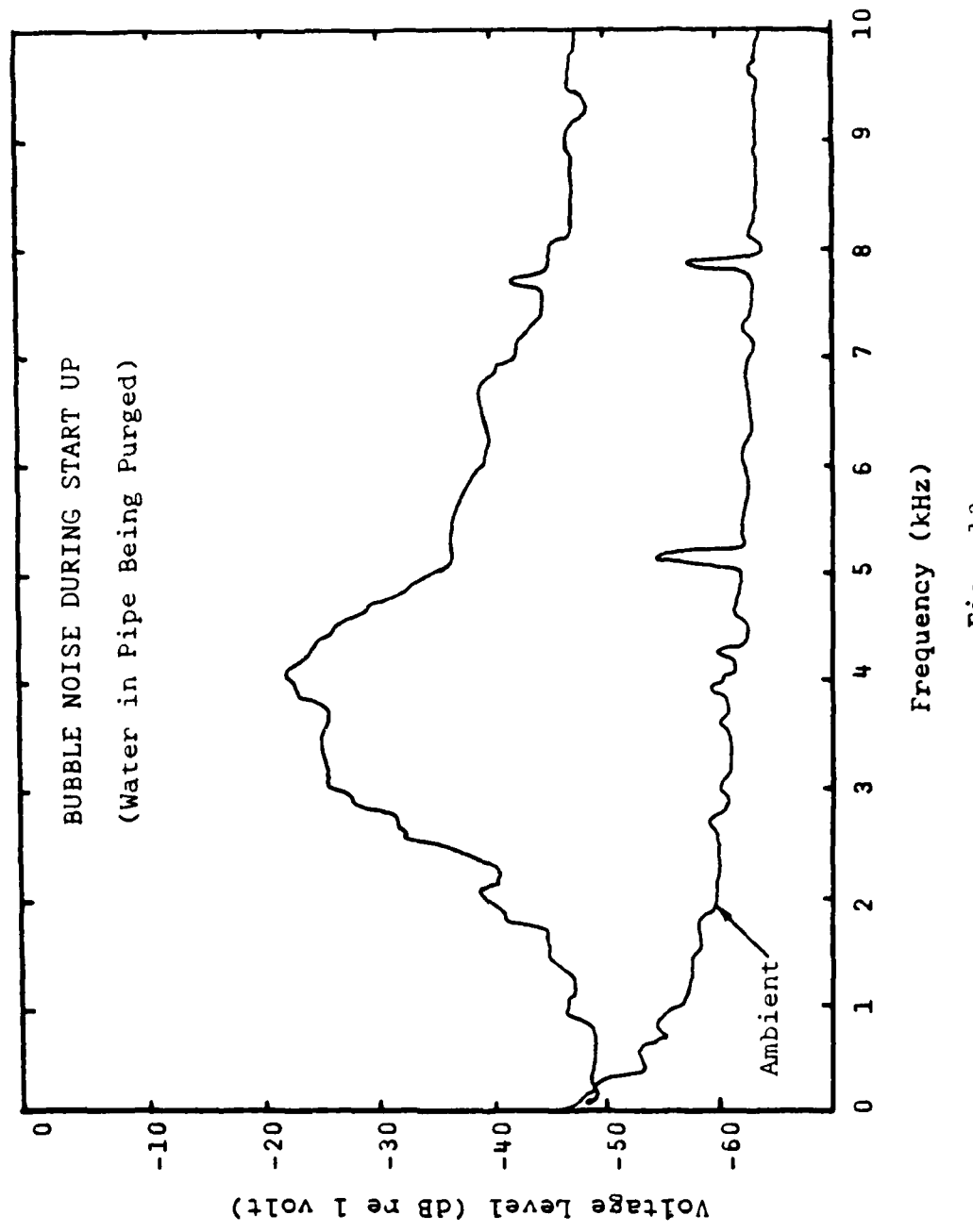


Fig. 13

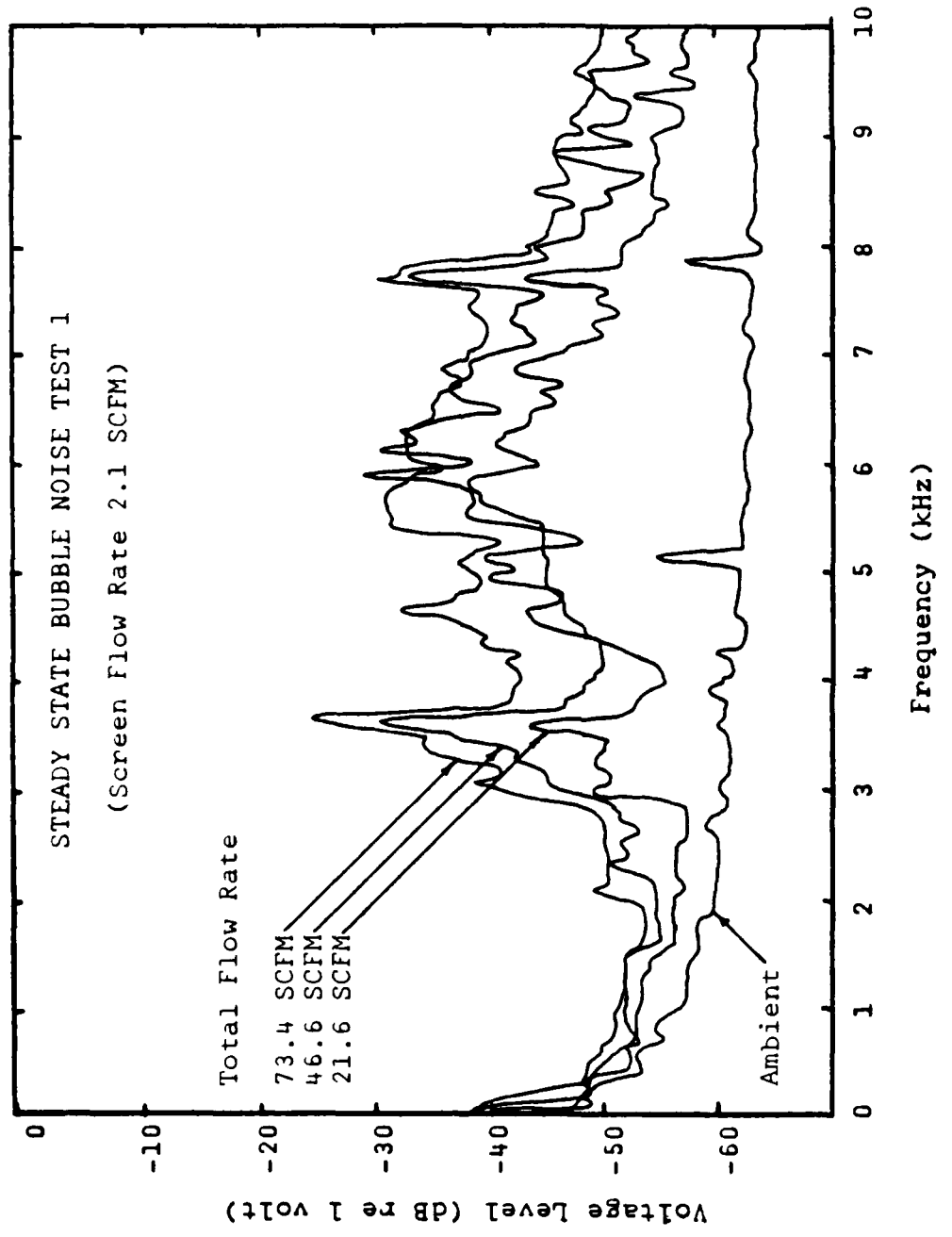


Fig. 14

TABLE VI. Bubble Screen Characteristics Data

Test No.	Rise Time (Still) (sec)	Rise Time (Turbulent) (sec)	Glass Box Fill Time (min)	Screen Thickness (cm)	Bubble Radius (cm)	Estimated Concentration (Ratio by volume of air to water) (percent)
1	7.0	4.4	3.7	10	0.25	2.1
2	6.1	4.0	1.7	15	0.3	4.6
3	5.7	3.9	1.4	20	0.2-0.4	5.6
4	4.5	2.5	3.2	17	0.4	2.5
5	3.9	2.4	1.4	25	0.5	5.6
6	3.7	2.4	0.9	27	0.3-0.6	8.7
7	7.0	5.3	9.4*	7	0.25	0.4
8	6.6	5.0	7.8	7	0.3	1.0
9	6.3	5.0	6.3	8	0.2-0.4	1.2

* Glass box turned lengthwise to reduce fill time.

TABLE VII. Tabulated Power in One-Third Octave Bands for Signal + Noise

Hz	K_L	K_R	K_C	K_{AV}	Test 1					Test 2					Test 3					Test 4.					Thres-		
					Watts	w	Watts	w	Watts	w	Watts	w	Watts	w	Watts	w	Watts	w	Watts	w	Watts	w	Watts	w	Watts	w	
25	0.22	0.22	0.05	0.16	0.39	0.32	0.19	0.39	0.32	0.39	0.32	0.32	0.32	0.32	0.32	0.39	0.39	0.32	0.39	0.32	0.39	0.32	0.39	<0.10	0.39		
31.5	0.28	0.28	0.12	0.23	0.43	0.61	0.43	0.37	0.32	0.43	0.19	0.15	0.15	0.15	0.15	0.32	0.32	0.15	0.32	0.15	0.32	0.15	0.32	<0.08	0.32		
40	0.36	0.36	0.23	0.32	0.22	0.10	0.14	0.39	0.22	0.22	0.22	0.10	0.08	0.10	0.08	0.10	0.10	0.10	0.10	0.10	0.10	0.10	0.10	0.10	<0.03	0.10	
50	0.47	0.47	0.42	0.45	0.20	0.20	0.26	1.78	0.31	0.24	0.20	0.18	0.20	0.20	0.18	0.20	0.20	0.20	0.20	0.20	0.20	0.20	0.20	<0.01	0.01		
62.5	0.63	0.63	0.63	0.63	1.1	1.1	1.1	2.5	1.2	1.2	1.2	1.1	1.1	1.1	1.1	1.1	1.1	1.1	1.1	1.1	1.1	1.1	1.1	1.1	1.1	<0.24	0.24
79.5	0.45	0.45	0.60	0.5	0.16	0.09	0.13	4.8	0.64	0.81	0.81	0.7	0.7	0.7	0.7	0.7	0.7	0.7	0.7	0.7	0.7	0.7	0.7	0.7	<0.03	0.03	
100	0.22	0.22	0.34	0.26	0.59	0.21	0.33	12.0	5.3	4.5	4.5	0.15	0.18	0.18	0.15	0.15	0.15	0.15	0.15	0.15	0.15	0.15	0.15	0.15	<0.07	0.07	
125	0.21	0.21	0.22	0.21	0.91	0.66	0.73	38	22	22	22	0.91	1.4	1.4	1.4	1.4	1.4	1.4	1.4	1.4	1.4	1.4	1.4	1.4	1.4	<0.3	0.3
157	0.16	0.16	0.11	0.14	8.2	5.6	4.1	86	51	3.4	3.4	4.0	3.4	3.4	3.4	3.4	3.4	3.4	3.4	3.4	3.4	3.4	3.4	3.4	<1.4	1.4	
200	0.16	0.16	0.075	0.13	21	21	100	130	12	12	12	10	10	10	10	10	10	10	10	10	10	10	10	10	<4.9	4.9	
250	0.13	0.13	0.075	0.11	3.3	1.9	3.3	83	100	83	100	83	100	83	100	83	100	83	100	83	100	83	100	83	<4.9	4.9	
315	0.15	0.15	0.037	0.11	1.6	0.14	3.3	10	21	13	13	13	13	13	13	13	13	13	13	13	13	13	13	13	<0.4	0.4	
400	0.15	0.15	0.040	0.23	0.19	0.19	0.19	0.43	1.7	1.18	1.18	0.27	0.27	0.27	0.27	0.27	0.27	0.27	0.27	0.27	0.27	0.27	0.27	0.27	<0.05	0.05	
500	0.10	0.10	0.059	0.09	1.2	1.2	1.2	1.2	1.2	1.2	1.2	1.2	1.2	1.2	1.2	1.2	1.2	1.2	1.2	1.2	1.2	1.2	1.2	1.2	<0.4	0.4	
625	0.10	0.10	0.059	0.09	1.0	1.0	1.0	1.5	2.8	2.8	2.8	11	9.7	9.7	11	9.7	9.7	11	9.7	9.7	11	9.7	9.7	11	<0.20	0.20	
795	0.14	0.14	0.11	0.13	0.59	1.2	1.3	3.4	21	15	15	15	0.72	1.0	1.0	1.0	0.72	1.0	1.0	1.0	0.72	1.0	1.0	1.0	<0.08	0.08	
1,000	0.13	0.13	0.11	0.13	0.48	1.2	1.2	1.9	2.4	15	15	15	15	1.0	1.0	1.0	1.0	1.0	1.0	1.0	1.0	1.0	1.0	1.0	<0.06	0.06	
1,250	0.21	0.21	0.17	0.20	0.16	0.49	1.0	1.0	1.3	1.3	1.3	1.3	1.3	1.3	1.3	1.3	1.3	1.3	1.3	1.3	1.3	1.3	1.3	1.3	<0.02	0.02	
1,570	0.22	0.22	0.24	0.23	0.12	0.76	0.91	1.0	9.3	9.3	9.3	9.3	0.61	0.61	0.61	0.61	0.61	0.61	0.61	0.61	0.61	0.61	0.61	0.61	<0.01	0.01	
2,000	0.22	0.22	0.23	0.22	0.10	0.53	1.0	1.0	1.0	1.0	1.0	1.0	1.0	1.0	1.0	1.0	1.0	1.0	1.0	1.0	1.0	1.0	1.0	1.0	<0.01	0.01	
2,500	0.37	0.37	0.20	0.32	0.035	0.32	0.88	3.0	88	77	77	77	2.0	4.8	4.8	2.0	4.8	4.8	2.0	4.8	4.8	2.0	4.8	4.8	2.0	<0.001	0.001
3,150	0.70	0.70	0.37	0.59	0.014	0.18	0.87	7.4	180	140	140	140	4.1	11	11	4.1	11	11	4.1	11	11	4.1	11	11	4.1	<0.002	0.002
4,000	0.99	0.99	0.81	0.93	0.009	0.23	1.2	3.7	74	49	49	49	2.3	4.6	4.6	2.3	4.6	4.6	2.3	4.6	4.6	2.3	4.6	4.6	2.3	<0.001	0.001
5,000	0.73	0.73	0.44	0.63	0.049	1.1	8.2	4.9	63	44	44	44	2.5	5.7	5.7	2.5	5.7	5.7	2.5	5.7	5.7	2.5	5.7	5.7	2.5	<0.002	0.002
6,250	0.49	0.49	0.32	0.43	0.49	1.4	4.4	1.9	22	22	22	22	1.5	2.7	2.7	1.5	2.7	2.7	1.5	2.7	2.7	1.5	2.7	2.7	1.5	<0.008	0.008
7,950	0.53	0.53	0.21	0.42	0.51	1.4	2.4	1.7	5.7	5.7	5.7	5.7	1.3	9.6	9.6	1.3	9.6	9.6	1.3	9.6	9.6	1.3	9.6	9.6	1.3	<0.010	0.010
10,000	0.70	0.70	0.46	0.62	0.10	0.40	0.40	0.40	0.65	0.65	0.65	0.65	0.14	0.40	0.40	0.14	0.40	0.40	0.14	0.40	0.40	0.14	0.40	0.40	0.14	<0.008	0.008

TABLE VIII. Tabulated Power in One-Third Octave Bands for Signal Alone

Test Numbers

Freq.	1	2	3	4	5	6	7	8	9
Hz	μW								
25	<0.10	<0.10	<0.10	<0.10	<0.10	<0.10	<0.10	<0.10	<0.10
31.5	0.11	0.29	0.11	<0.08	<0.08	0.11	<0.08	<0.08	<0.08
40	0.12	<0.03	0.04	0.29	0.12	0.12	<0.03	<0.03	<0.03
50	0.15	0.15	0.21	1.7	0.26	0.19	0.15	0.13	0.15
62.5	<0.24	<0.24	<0.24	1.4	0.30	0.30	<0.24	<0.24	<0.24
79.5	0.05	<0.03	0.04	4.7	0.55	0.72	<0.03	<0.03	<0.03
100	0.34	<0.07	0.07	12	5.0	4.2	<0.07	<0.07	<0.07
125	<0.30	<0.30	<0.30	37	21	21	<0.30	<0.30	<0.30
157	3.0	<1.4	<1.4	36	81	46	<1.4	<1.4	<1.4
200	<4.9	<4.9	<4.9	82	110	110	<4.9	<4.9	<4.9
250	1.9	0.50	1.9	82	99	82	0.70	0.50	0.50
315	<0.40	<0.40	1.7	8.0	19	11	<0.40	<0.40	<0.40
400	<0.05	<0.05	<0.05	2.4	1.5	1.0	0.08	<0.05	0.13
500	<0.40	<0.40	<0.40	1.6	6.5	10	0.90	0.90	1.2
625	0.40	0.90	0.90	2.2	10	9.0	0.90	0.90	1.2
795	0.30	0.90	1.0	3.1	21	15	0.40	0.70	0.70
1,000	0.27	1.0	1.7	2.2	15	15	0.80	1.7	1.1
1,250	0.07	0.40	0.90	1.2	12	7.5	0.62	0.80	1.2
1,570	0.07	0.29	0.44	1.0	9.3	9.3	0.56	0.86	2.3
2,000	0.05	0.48	1.0	1.9	35	35	1.5	2.5	1.3
2,500	0.01	0.30	0.86	3.0	88	77	2.0	4.8	2.2
3,150	0.007	0.17	0.86	7.4	180	140	4.1	11	5.8
4,000	0.005	0.23	1.2	3.7	74	49	2.3	4.6	3.5
5,000	0.04	1.1	8.2	4.9	63	44	2.5	5.7	5.1
6,250	0.46	1.4	4.4	1.9	22	22	1.1	2.7	2.2
7,950	0.46	1.4	2.4	1.7	5.7	8.2	0.53	1.3	9.6
10,000	0.07	0.37	0.37	0.37	0.62	0.62	0.11	0.37	1.5

TABLE IX. Source Level (dB re 1 μ Pa) for One-Third Octave Bands

Freq.

	Hz	1	2	3	4	5	6	7	8	9	Thres-hold
-	25	<101.5	<101.5	<101.5	<101.5	<101.5	<101.5	<101.5	<101.5	<101.5	101.5
31.5	101.9	106.1	101.9	100.5	100.5	101.9	<100.5	<100.5	<100.5	<100.5	101.5
40	102.3	<96.3	97.5	106.1	102.3	102.3	<96.3	<96.3	<96.3	<96.3	96.3
50	103.3	103.3	104.7	113.9	105.6	104.3	103.3	102.6	103.3	103.3	91.5
62.5	<105.3	<105.3	<105.3	113.0	106.3	106.3	<105.3	<105.3	<105.3	<105.3	105.3
79.5	98.5	<96.3	97.5	118.2	108.9	110.1	<96.3	<96.3	<96.3	<96.3	96.3
100	106.8	<100.0	100.0	122.2	118.5	117.7	<100.0	<100.0	<100.0	<100.0	100.0
125	<106.3	<106.3	<106.3	127.2	124.7	124.7	<106.3	<106.3	<106.3	<106.3	106.3
157	116.3	<113.0	<113.0	127.1	130.6	128.1	<113.0	<113.0	<113.0	<113.0	113.0
200	<118.4	<118.4	<118.4	130.6	132.0	132.0	<118.4	<118.4	<118.4	<118.4	118.4
250	114.3	108.5	114.3	130.6	131.5	130.6	110.0	108.5	108.5	108.5	107.5
315	<107.5	<107.5	113.8	120.5	124.3	121.9	<107.5	<107.5	<107.5	<107.5	107.5
400	<98.5	<98.5	<98.5	115.3	113.3	111.5	100.5	<98.5	<98.5	<98.5	<98.5
500	<107.5	<107.5	<107.5	113.5	119.5	121.5	111.0	111.0	112.3	112.3	107.5
625	107.5	111.0	111.0	114.9	121.5	121.0	111.0	111.0	112.3	112.3	104.5
795	106.3	111.0	111.5	116.4	124.7	123.3	107.5	107.5	110.0	110.0	100.5
1,000	105.8	111.5	113.8	114.9	123.3	123.3	110.5	113.8	111.9	111.9	99.3
1,250	100.0	107.5	111.0	112.3	122.3	120.3	109.4	110.5	112.3	112.3	94.5
1,570	100.0	106.1	107.9	111.5	121.2	121.2	109.0	110.8	115.1	115.1	91.5
2,000	98.5	108.3	111.5	114.3	126.9	113.3	115.5	115.5	122.6	122.6	91.5
2,500	91.5	106.3	110.8	116.3	130.9	130.4	114.5	118.3	124.9	124.9	81.5
3,150	90.0	103.8	110.8	120.2	134.1	133.0	117.6	121.9	129.1	129.1	84.5
4,000	88.5	105.1	112.3	117.2	130.2	128.4	115.1	118.1	126.9	126.9	81.5
5,000	97.5	111.9	120.6	118.4	129.5	127.9	115.5	119.1	128.6	128.6	84.5
6,250	108.1	113.0	117.9	114.3	124.9	124.9	111.9	115.8	124.9	124.9	90.5
7,950	108.1	113.0	115.3	113.8	119.1	120.6	108.7	112.6	121.3	121.3	91.5
10,000	100.0	107.2	107.2	107.2	109.4	109.4	101.9	107.2	113.3	113.3	90.5

V. DISCUSSION OF RESULTS

A. GENERAL TRENDS

Examination of the 170 graphs for qualitative results was the first phase of analysis. An expected finding was that as the pressure was increased the noise increased. This is shown in Fig. 7, 8, and 9 for example. Also expected was that as the hole size increased the noise likewise increased. This can be seen by comparing test seven to test four in Fig. 9 and Fig. 8 respectively. An unexpected but very significant finding was that for test one as compared to test seven, (Fig. 7 and 9) the noise was overall six decibels less for test one even though it was producing five times the flow rate. However, above five kilohertz the noise produced in test one was higher by six decibels on the average with a peak of twelve decibels at about six kilohertz. This can be explained as the same phenomenon that occurs in masker systems. Since the bubbles completely surround the pipe, they are masking the noise of generation in the frequency range from about 0.5 kilohertz to five kilohertz due to bubble resonance. Referring to Tables I and VI one sees that the bubble radius for test one corresponds to resonance at these frequencies with the peak resonance occurring near two kilohertz. The fact that the noise power

is only four times as great in the upper frequencies may be attributed to some masking occurring due to bubble interaction and reflection at these upper frequencies. Similar results can be seen with examination of tests two and three compared to tests eight and nine respectively in the above mentioned figures. Test two however, is lower in noise in the two to five kilohertz range, but approximately equal elsewhere. Test three had a larger variation in bubble size which accounts for reduced noise over a slightly broader range.

Before comparing tests one through three with tests four through six it is necessary to examine the flow rates given in Table IV. Choosing flow rates of approximately equal value for the two basic hole sizes one can see that tests one and four nearly coincide and tests three and five correspond exactly. Analysis of Fig. 7 and 8 shows that overall there is considerably less noise with pipe one. In fact comparing test one with test four there is a twenty decibel reduction. Only between 5.5 and 7.5 kilohertz does test one noise level exceed that of test four and then only by a maximum of five hertz. Though the effect is not as dramatic, test three is also less than test five in overall level. However, test three does exceed it in the above five kilohertz range by an average of four decibels.

In order to compare screening characteristics of the various tests, one must know the ratio of air to water by

volume. The values given in Table IV were calculated by dividing the height of rise by the rise time to get speed, finding the volume exchanged on one second for a unit width screen based on the speed, finding the amount of air introduced into this volume per second using the previously calculated flow rate, and finally dividing the air volume by the total volume to give a ratio.

Examination of Table VI shows that the concentrations for tests one and three are higher than for tests four and five respectively even though flow rates are about equal. This is due to the greater screen thickness of tests four and five.

Fig. 10 tends to support the conclusion that the major portion of the noise is produced during the generation of the bubbles. Test six shows this most clearly. However, all eight other sets of graphs show a similar pattern. Examination of Fig. 10 shows that in fact the noise produced during bubble formation is on the average ten decibels higher with a peak of fifteen decibels higher between three and five kilohertz. The second most significant noise appeared to be that generated during their ascent. Fig. 11 and 12 show an expanded look at the range of frequencies from 0 - 500 hertz. The data are contaminated with components from power line noise at sixty hertz and its harmonics. This noise could not be reduced further with the available equipment even though considerable effort was made in shielding

all wires and grounding all equipment. Despite this noise, a general trend can be seen. Test one shows a peak increase of nine decibels above background noise at the 200 hertz frequency. An additional ten decibels increase is seen when comparing test one with four showing that test one is also quieter within this range. For the #80 drill holes the signal to noise level was so low that useful information could not be derived from the 0 - 500 hertz range other than the fact that noise produced in tests seven, eight and nine was very low in this range of frequencies.

Fig. 14 shows components associated with valve flow noise. The peak in the 7.5 kilohertz range was identified during experimentation as the valve throttling noise of the inlet valve, and the peak in the four kilohertz range was identified as the exit valve throttling noise. Both of these noises are artifacts associated with the particular valve. These would be eliminated by careful design of the air flow control system. Therefore, the noise from flow through the pipe appears to be evenly distributed from two to ten kilohertz. If a large diameter pipe were used the air speed through the pipe would be reduced. The speed therefore is the critical factor to the noise. Pipe diameters for an actual screen must be large enough to permit conditions to approach that of a reservoir throughout the entire screen length.

B. ACOUSTIC POWER

Eq. (2), (3), and (4) were used to tabulate the values in Table VII. The acoustic power is listed in microwatts in each one-third octave band for the entire 4.83 foot screen for the various tests. Test ten is for ambient noise level or "noise" while the other entries are for "signal". If signal to noise ratio was less than satisfactory a threshold level was applied to indicate that the signal was somewhat less than the threshold value. The threshold value was arrived at by assuming maximum probable error in reading the meter level was one decibel. The threshold value was calculated by

$$\text{Threshold} = (1.27 \times \text{noise power}) - \text{noise power} \quad (7)$$

Table VIII contains the values of power for each steady state test of the bubble screen.

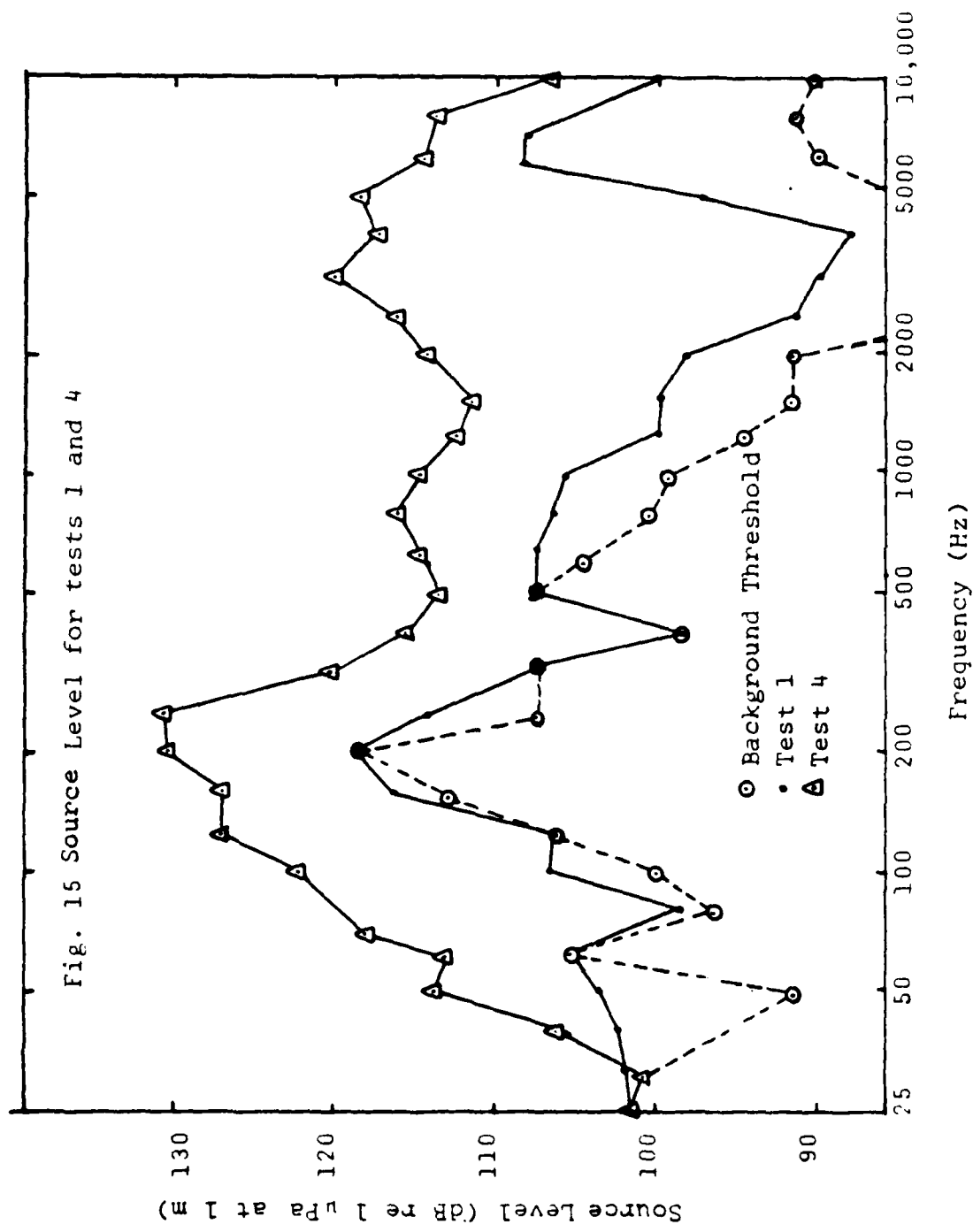
The values in Table IX are calculated from the information contained in Table VIII and from Eq. 2. It is assumed that the screen can be treated as an equivalent point source. The noise power in each one-third octave band is used to calculate a source level for a non-directional source.

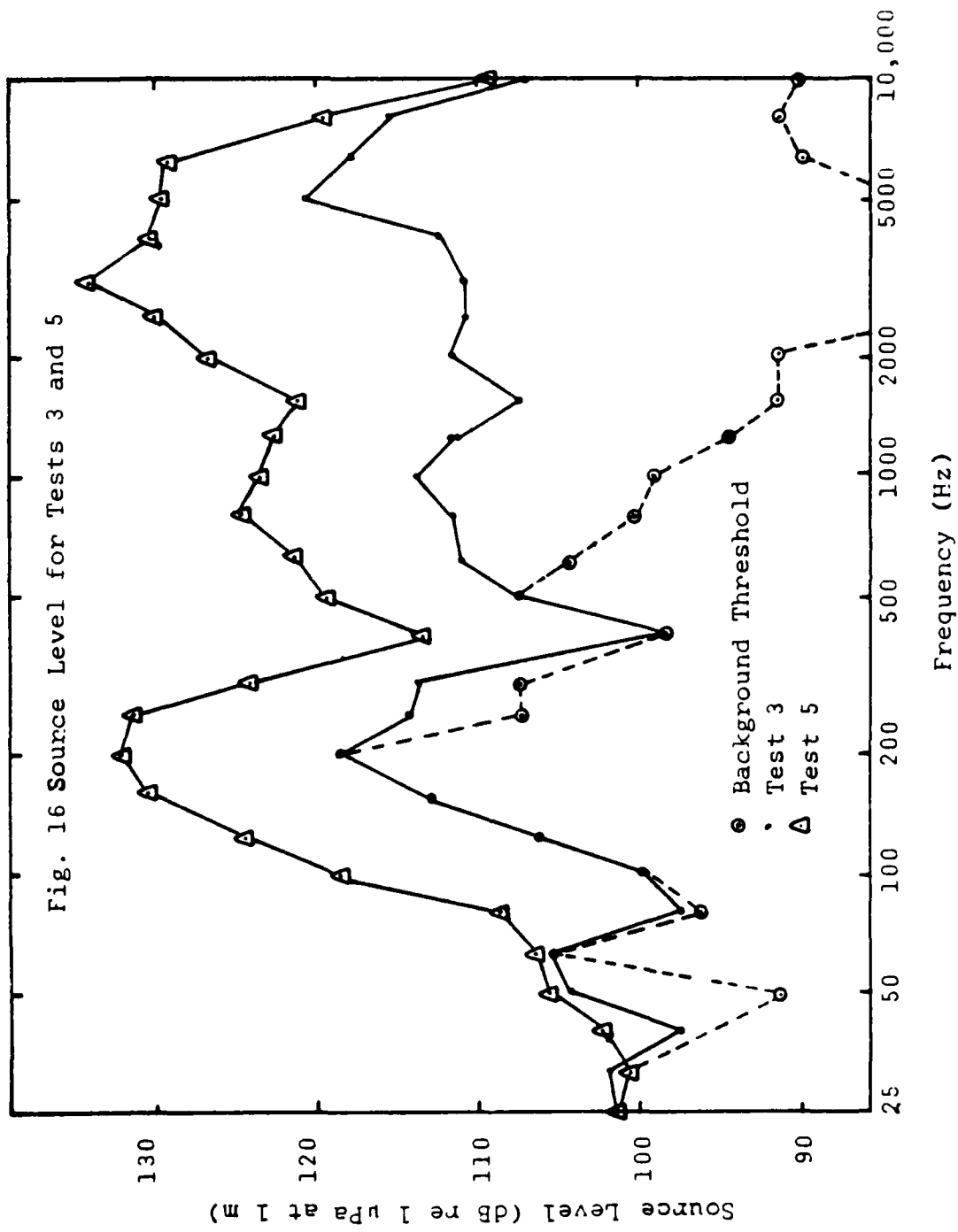
IV. CONCLUSIONS AND RECOMMENDATIONS

Pipe configuration one (a large number of very small holes spaced around the pipe) with one PSI pressure differential produces a very uniform acoustic bubble screen at the lowest sound level of any of the tests. Fig. 15 compares test one with test four (pipe 2 - one row of larger holes), which had similar flow rates. For test one, the source level is thirty decibels lower in the two to five kilohertz range, with an average of ten decibels lower throughout the remaining frequencies. Furthermore, the screen density for test one was within acceptable limits.

Perhaps the masking effect of the bubbles surrounding the pipe during generation was responsible for the significant reduction in noise through the frequency range for higher flow rates as well as the lower flow of test one. Examination of Fig. 16 shows that test three also averages ten decibels lower in source level. However, the sharp decrease in the two to five kilohertz range is no longer present. The results of test three show that if higher flow rates are demanded from configuration one, the noise continued to remain lower than the same flow rate produced by pipe configuration two. The masking effect of the bubbles surrounding the pipe when configuration one was used may contribute significantly to noise reduction at all flow rates.

Fig. 15 Source Level for tests 1 and 4





Another advantage of configuration one is that water inside the pipe is more quickly discharged since a large percentage of the holes are on the underside of the pipe, and gravity tends to cause water to exit primarily through holes on the bottom.

Screen persistance is greater with configuration one since the bubbles rise more slowly due to their smaller size. Water turbulence is also reduced for the same reason, which may account for a small fraction of the noise reduction.

One disadvantage to configuration one is that the screen thickness is less than for configuration two and a wider screen would require multiple generators placed side by side.

A larger pipe would be required for any practical screen since air velocity must be kept low in the pipe. It seems quite possible that a six-inch pipe with the same seven rows of holes of #80 drill would produce similar noise results. However, actual experimentation with larger sizes was not feasible.

The results of this paper tend to support the recommendation that generation of a bubble screen with a minimum of induced noise should be done with orifices on the order of 0.014 inches in diameter and with a configuration that provides for air completely surrounding the generator as it is produced. Further study to determine effects of depth on noise, effects of increased pipe size and pipe length,

and effects of multiple generators to increase screen thickness by a future thesis student would answer some of the remaining questions concerning noise produced by an acoustic bubble screen.

LIST OF REFERENCES

1. Carstensen, E. L. and Foldy, L. L., "Propagation of Sound Through a Liquid Containing Bubbles," The Journal of the Acoustical Society of America, v. 19, p. 481-500, May 1947.
2. David Taylor Model Basin Hydromechanics Laboratory Research and Development Report C-805, Criteria for the Design of Bubble-Screening Systems for the Suppression of Underwater Sound with Particular Application to Minesweepers, by S. F. Crump, p. 2-10, February 1957.
3. Clay, C. S. and Medwin, H., Acoustical Oceanography, John Wiley & Sons, 1977.
4. Wood, A. B., A Testbook of Sound, p. 360-363, The MacMillan Company, 1941.
5. Strasberg, M., "Gas Bubbles as Sources of Sound in Liquids," The Journal of the Acoustical Society of America, v. 28, p. 20-26, January 1956.
6. Datta, R. L., Napier, D. H., and Newitt, D. M., "The Properties and Behavior of Gas Bubbles Formed at a Circular Orifice," Institution of Chemical Engineers, Transactions,
7. NRDC Summary Technical Report, Physics of Sound in the Sea, ed. R. Wildt, v. 8, chap. 28, p. 460-477, 1946.

INITIAL DISTRIBUTION LIST

	No. Copies
1. Defense Technical Information Center Cameron Station Alexandria , Virginia 22314	2
2. Library, Code 0142 Naval Postgraduate School Monterey, California 93940	2
3. Department Chairman, Code 61 Department of Physics and Chemistry Naval Postgraduate School Monterey, California 93940	1
4. Professor O. B. Wilson, Jr., Code 61 W1 Department of Physics and Chemistry Naval Postgraduate School Monterey, California 93940	4
5. Professor J. V. Sanders, Code 61 Sd Department of Physics and Chemistry Naval Postgraduate School Monterey, California 93940	1
6. LT C. T. Kelley, USN 1812 Longmeadow Drive Montgomery, Alabama 36106	1
7. Commander Puget Sound Naval Shipyard ATTN: Carr Inlet Acoustic Range Branch Code 246 Bremerton, Washington 98314	10
8. LT K. W. Marr, USN 2636 N. Seventh Street Sheboygan, Wisconsin 53081	1

